

**MULTIPATH EXPLOITATION IN THROUGH-
WALL RADAR IMAGING USING SPARSITY-
DRIVEN DETECTION**

BY

ALI ATTYATULLAH ALBELADI

A Thesis Presented to the
DEANSHIP OF GRADUATE STUDIES

KING FAHD UNIVERSITY OF PETROLEUM & MINERALS

DHAHRAN, SAUDI ARABIA

In Partial Fulfillment of the
Requirements for the Degree of

MASTER OF SCIENCE

In

ELECTRICAL ENGINEERING

May, 2015

KING FAHD UNIVERSITY OF PETROLEUM & MINERALS
DHAHRAN- 31261, SAUDI ARABIA
DEANSHIP OF GRADUATE STUDIES

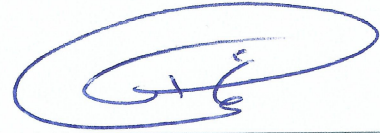
This thesis, written by Ali Attyatullah AlBeladi under the direction his thesis advisor and approved by his thesis committee, has been presented and accepted by the Dean of Graduate Studies, in partial fulfillment of the requirements for the degree of **MASTER OF SCIENCE IN ELECTRICAL ENGINEERING.**



Dr. Ali Muqaibel
(Advisor)



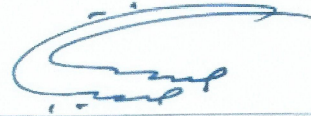
Dr. Ali Al-Shaikhi
Department Chairman



Dr. Ali Al-Shaikhi
(Member)



Dr. Salam A. Zummo
Dean of Graduate Studies



Dr. Tareq AlNaffouri
(Member)

28/5/13

Date

© Ali AlBeladi

2015

*To my Compassionate Mother
& my Caring Father*

ACKNOWLEDGMENTS

[All Praise to Allah the Most Compassionate, the Most Gracious. Him alone I thank for all the blessings that He bestowed upon me.

My utmost gratitude goes to my wonderful parents for always giving me confidence in myself and for their endless support and prayers throughout my life. Nothing I say or do can pay them back, I am so lucky to have such parents. I would also like to thank my great brothers and sisters for their support and encouragement. Special thanks to my beloved wife for her patience, understanding, and for being there for me in tough situations.

I would like to convey my sincere gratitude to my thesis advisor Dr. Ali Hussein Muqaibel for his support and guidance. I thank him for being available whenever I needed his assistance. I have learned a lot from him, both academically and morally. It is my pleasure working with him.

Special thanks to the members of my thesis committee Dr. Ali Al-Shaiki and Dr. Tareq AlNaffouri for their useful guidance, motivation, and professional contribution to my success and that of this work.

I was lucky to have Abu Taleb, Abu Salem, and Mohammad Tamim with me throughout my research work. I acknowledge them for their support and help as well as their enriching discussions; I have learned from them a lot. Finally I thank KFUPM for the opportunity it gave me to accomplish this work.]

TABLE OF CONTENTS

| | |
|-----------------------------------|------|
| ACKNOWLEDGMENTS | V |
| TABLE OF CONTENTS..... | VI |
| LIST OF TABLES..... | X |
| LIST OF FIGURES | XI |
| LIST OF ABBREVIATIONS | XIII |
| ABSTRACT | XV |
| ملخص الرسالة | XVII |
| CHAPTER 1: INTRODUCTION..... | 1 |
| 1.1 Overview | 1 |
| 1.2 Literature Review..... | 2 |
| 1.2.1 Change Detection | 3 |
| 1.2.2 Compressive Sensing | 4 |
| 1.2.3 Multipath Exploitation..... | 6 |
| 1.3 Thesis Contribution | 8 |
| 1.4 Thesis Organization | 9 |

| | | |
|--|---|-----------|
| 1.5 | Notation..... | 10 |
| CHAPTER 2: BACKGROUND | | 11 |
| 2.1 | Overview | 11 |
| 2.2 | Through-the-Wall Impulse Radar..... | 12 |
| 2.3 | Moving Objects Indication Using Change Detection | 14 |
| 2.4 | Challenges in TWRI..... | 15 |
| 2.4.1 | Front Wall Effect..... | 15 |
| 2.4.2 | Multipath Effect | 17 |
| 2.5 | Imaging Techniques | 18 |
| 2.5.1 | Back-Projection | 19 |
| 2.5.2 | CS-Based TWRI | 20 |
| CHAPTER 3: EVALUATING COMPRESSIVE SENSING ALGORITHMS IN THROUGH-THE-WALL RADAR VIA F1-SCORE | | 23 |
| 3.1 | Introduction..... | 23 |
| 3.2 | CS in TWRI | 27 |
| 3.2.1 | Sparse Reconstruction..... | 27 |
| 3.2.2 | Compressing Data Via CS | 30 |
| 3.3 | Evaluation Criterion | 31 |

| | | |
|---|--|-----------|
| 3.4 | Results and Discussion | 34 |
| 3.4.1 | Detection Performance vs. SNR | 35 |
| 3.4.2 | Detection Performance vs. Compression Rate | 36 |
| 3.4.3 | Regions of desired performance | 39 |
| 3.5 | Conclusion | 40 |
| | | |
| CHAPTER 4: JOINT WALL POSITION DETECTION AND MULTIPATH | | |
| EXPLOITATION IN TWRI | | |
| | | 41 |
| 4.1 | Introduction..... | 41 |
| 4.2 | Multipath Model..... | 42 |
| 4.3 | In Pursuit of the Wall Positions..... | 44 |
| 4.3.1 | General Framework..... | 44 |
| 4.3.2 | Variations in the Proposed Wall Pursuit (WP) Framework | 48 |
| 4.4 | Basic WP Algorithm | 49 |
| 4.4.1 | Variations clarified..... | 49 |
| 4.4.2 | Results and Discussion | 50 |
| 4.5 | Dynamic Wall Pursuit (DWP) Algorithm | 54 |
| 4.5.1 | Extensions to WP | 54 |
| 4.5.2 | Results and Discussion: | 55 |
| 4.6 | Conclusion | 59 |

| | |
|--|-----------|
| CHAPTER 5: CONCLUSION AND RECOMMENDATIONS | 60 |
| 5.1 Conclusion | 60 |
| 5.2 Recommendations for Future Research | 62 |
| REFERENCES..... | 64 |
| VITAE | 74 |

LIST OF TABLES

| | |
|--|----|
| Table 1.1: CS Algorithms Used in TWRI Literature | 6 |
| Table 1.2: Notation used throughout the thesis | 10 |
| Table 3.1: CS Algorithms Evaluated | 26 |

LIST OF FIGURES

| | |
|--|----|
| Figure 2.1: Simple geometry of the scene..... | 13 |
| Figure 2.2: Scene geometry in TWRI showing the effect of the front wall..... | 16 |
| Figure 2.3: The geometry of the scene including the multipath signals..... | 18 |
| Figure 3.1: Geometry of the scene..... | 27 |
| Figure 3.2: Performance of CS algorithms when varying the SNR, (a) all the data is used, (b) 10% of the data is used (for clarity, only the 9 algorithms are shown)..... | 36 |
| Figure 3.3: Performance of CS algorithms when varying the size of the measurement matrix, SNR = (a) -10 dB, (b) 30 dB (for clarity, only the 9 algorithms with best performances are shown)..... | 38 |
| Figure 3.4: Algorithms region of desired performance ($F1 \geq 0.9$) (for image convenience, only the 6 algorithms with best performances are shown)..... | 39 |
| Figure 4.1: The block diagram of the Wall Pursuit general framework..... | 47 |
| Figure 4.2: (a) Percentage of successfully detecting the walls with variation in SNR (dB), (b) The status of the algorithm at the end for each SNR. | 52 |
| Figure 4.3: The average level of depth needed to achieve the success rate given in Figure 4.2 (a)..... | 53 |

| | |
|---|----|
| Figure 4.4: A comparison between the two proposed algorithms with respect to the percentage of successfully detected walls, with variation in SNR (dB)..... | 56 |
| Figure 4.5: The average number of frames needed to achieve the success rate given in Figure 4.4 (a) | 57 |
| Figure 4.6: Histogram of number of frames needed for successful wall detection SNR = (a) 10, (b) 15, and (c) 20 | 58 |

LIST OF ABBREVIATIONS

| | |
|------|--|
| CD | Change Detection |
| CFAR | Constant false alarm rate |
| CS | Compressive Sensing |
| DWP | Dynamic Wall Pursuit |
| MDG | Multipath dictionary generator |
| MIMO | Multiple-input multiple-output |
| MP | Multipath |
| PSF | Point spread function |
| SCR | Signal-to-clutter ratio |
| SFCW | Stepped-frequency continuous-wave |
| SVD | Singular Value Decomposition |
| TSVD | Truncated Singular Value Decomposition |
| TWRI | Through-wall radar imaging |
| UWB | Ultra-wideband |

WP

Wall Pursuit

|

ABSTRACT

Full Name : Ali Attyatullah AlBeladi

Thesis Title : Multipath Exploitation in Through-Wall Radar Imaging Using
Sparsity-Driven Detection

Major Field : Digital Signal Processing

Date of Degree: May, 2015

To achieve a high resolution Through-the-Wall Radar Image (TWRI), massive amounts of data is acquired. Compressive Sensing (CS) techniques resolve this issue by allowing image reconstruction using much fewer measurements. The performance of different CS algorithms, when applied to TWRI, has not been investigated in a comprehensive and comparative manner. In this thesis, popular CS algorithms are evaluated in terms of their detection capabilities, to see which are most suitable for TWRI applications. As for the evaluation criteria, the notion of F_1 -score is adopted and used. Algorithms responses to different levels of SNR and compression rate are evaluated. Numerical results show that for systems with low SNR, alternating direction based algorithms work better than others.

With the aim of exploiting multipath reflections to enhance the image, a general framework that jointly detects the position of the inner walls and produces a ghost-free image of the scene of interest is introduced. Two algorithms are proposed within this framework. The first is the basic Wall Pursuit (WP) algorithm, which is a greedy-based wall searching method. The second, called the Dynamic Wall Pursuit

(DWP), extends the first method to include moving targets. The results show that making use of different time frames of the scene can be of significant help in gaining new information about the wall positions. |

ملخص الرسالة

الاسم الكامل: علي بن عطية الله البلادي

عنوان الرسالة: استغلال تعدد مسارات الإشارة في التصوير الراداري عبر الجدار باستخدام خاصية التناثر

التخصص: معالجة الإشارة الرقمية

تاريخ الدرجة العلمية: رجب 1436 هـ

لتحقيق دقة عالية في التصوير الراداري عبر الجدران لابد من الحصول على كمية هائلة من البيانات من ثم معالجتها وتخزينها. إن الاستعانة بتقنية الاستشعار المنضغط تعيننا على استخراج صورة ذات دقة عالية باستخدام كمية قليلة من البيانات ، هي أقل بكثير من تلك التي نحتاجها في الطرق المعتادة. ولهذه التقنية خوارزميات كثيرة ، ولم يتم التحق بعد في أيهم أنسب للتصوير الراداري عبر الجدران. في هذه الأطروحة تم تقييم بعض الخوارزميات الشائعة للاستشعار المنضغط من ناحية مدى قدرتهم على كشف الأجسام خلف الجدران عند استخدام التصوير الراداري. أما بالنسبة لمعيار التقييم ، فاعتمدنا بما يسمى درجـ F_1 والتي تعني بقدرة الخوارزمية على تحديد الأماكن التي بها أجسام بشكل صحيح. تم تقييم الخوارزميات تحت مستويات مختلفة من نسبة الإشارة إلى التشويش (SNR) ومن معدل الضغط.

كذلك قمنا باستحداث منهجية عامة لاستغلال الإشارات المنعكسة عبر الجدران الداخلية لتحديد أماكن الجدران وبالتالي تحسين الصورة النهائية للمشاهد المراد تصويره. تم اقتراح خوارزميتان داخل الإطار العام لهذه المنهجية ، الخوارزمية الأولى تعتمد على البحث على الموقع الأمثل للجدار في كل اتجاه ومن ثم تحديث الصفوفة بناء على نتيجة البحث ، يتم تكرار هذه العملية حتى نصل إلى المواقع الصحيح للجدران. أما الخوارزمية الثانية ، فهي إمتداد للأولى مع الإستفادة من الأجسام المتحركة داخل المشهد. أظهرت النتائج أن الاستفادة من الإشارات المرتدة عبر إطارات زمنية مختلفة تساعد على كشف أماكن الجدران الداخلية ، وذلك عند وجود أجسام متحركة.

CHAPTER 1: INTRODUCTION

1.1 Overview

Through-the-wall radar imaging (TWRI) is an emerging technology which gives the ability to see the contents of an indoor scene. During the past decade, this technology has witnessed a growing interest. TWRI is helpful in various civilian and military applications; for example, it can be used in determination of building layouts, behind-the-wall target detection, surveillance and investigation, rescue missions, and even in some medical applications. These features are highly desirable for a range of organizations, including police, rescue personnel, first responders, and defense forces. [1]

In such applications, providing timely actionable intelligence by reducing data acquisition and processing time is desirable. The number of targets in a scene is often small compared to the empty space, and thus the scene is said to be sparse. Hence, compressive sensing (CS) techniques can be applied to reconstruct the image of the desired scene. These techniques have the capability to recover a sparse signal from a far fewer number of measurements. CS has been shown to yield a great reduction in cost while maintaining reliable sensing efficiency in terms of resolution [2]. However, CS performance with application to TWRI has not been extensively

studied yet. In this thesis, the performance of various CS algorithms when applied to TWRI will be studied.

In many cases detecting human motion behind the walls is highly desirable, such as fire and hostage situations. Motion detection can be accomplished by subtracting two consecutive data frames and therefore suppressing returns from stationary objects and leaving the sparse scene with only the moving targets. This is called Change Detection (CD) technique.

In practical applications, the transmitted signal will mainly reflect from the walls, stationary objects, and the moving targets inside the room. Moreover, not all of the reflections return directly to the receiver. Some of them are received from an indirect path (e.g. signal reflects from a target to a side wall then back to the receiver). These signals are called multipath signals. Multipath signals are major sources of challenge in TWRI applications; the additional propagation time it takes the signal to return back to the receiver will be misinterpreted as a reflection of the signal from a further away target. This will result in the appearance of false targets in the reconstructed image, known as *multipath ghosts*. Methods for exploiting multipath signals resulting from moving targets will be presented in this thesis.

1.2 Literature Review

The research in hand covers three main topics, namely: change detection, compressive sensing, and multipath exploitation in TWRI. The literature review is organized accordingly.

1.2.1 Change Detection

One approach used to discriminate movements from background clutters is based on Doppler exploitation methods [1]. However, these methods are not practical for human targets because their motion is abrupt and non-stationary, which makes capturing the Doppler shift difficult [2]. Also, time-frequency analysis can be used to identify instantaneous frequency signatures [1]. However, time-frequency representations are often very complex to interpret [2]. Alternatively, CD can be used to suppress heavy clutter caused by reflections from stationary objects [3].

CD in TWRI has been implemented in ultra-wide band (UWB) random noise radar in [4]. The authors in [4] recognized moving targets through coherently subtracting successive frames of the cross-correlation between the transmitted and received signals. Then the resulting difference signal was used to obtain the image of the moving target using the back-projection imaging algorithm; this scheme is called coherent CD, where the image is formed after signal subtraction. Alternatively in [5], the image intensities for two consecutive frames in stepped-frequency continuous wave (SFCW) radar were first reconstructed, and then a positive threshold was applied to the difference between the images; this is called the intensity CD scheme, where the subtraction is done after image formation. Both Electromagnetic modeling simulation and experimental data were used to validate the methods in [4]. Later, this approach was further improved in [6] by making use of the phase change detection and applying the constant false alarm rate (CFAR) algorithm to determine the appropriate threshold. In [3], a comprehensive analytical treatment of multiple-input multiple-output (MIMO) CD was provided for both

coherent and intensity CD schemes described earlier. From their experimental results, it was concluded that the coherent CD scheme has better performance in detecting targets with small displacements.

1.2.2 Compressive Sensing

Driven by the challenges that TWRI systems face, such as prolonged data acquisition time and a huge amount of data, Huang *et al.* [7] proposed a data acquisition scheme and imaging algorithm for SFCW TWRI based on CS. The authors showed that more than 90% of the spatial and frequency measurements can be dropped without compromising the image quality. The same was later proposed for UWB impulse radar TWRI by Zhang *et al.* [8]. Instead of applying CS to reduce both spatial and frequency, the authors in [9] proposed a hybrid approach where they combined the CS approach with the truncated singular value decomposition (TSVD) inverse scheme presented in [10]. In their work, the CS approach was used to reduce the number of frequency measurements only, where the TSVD was used to reduce the number of spatial measurement points. Contrary to the CS only case, this approach provides significant reduction in data volume while maintaining good image quality. It is therefore preferred when we want to retain the characteristics of a back-projection image, particularly the decay of the imaged target intensity; which is not possible in the CS only case.

Most of the previous research implementing CS in TWRI assumes effective removal of wall backscattering before implementing CS. The authors in [11] applied the spatial filtering and subspace projection wall mitigation techniques with a reduced

set of measurements using CS. Using experimental data, they demonstrated that their method maintains acceptable performance. When implementing CS in detecting moving objects using CD, wall mitigation is not necessary; an attempt to reduce the data volume for CD using CS was given in [2]. The authors developed CD models for both translational motions and short sudden movements to allow scene reconstruction under CS framework. They showed through experiments that their approach had achieved a sizable reduction in the data volume without degradation in system performance. Another approach for detecting the presence of moving targets (but without localizing them) was proposed in [12], where a matrix of multiple measurements is formed and compressed using a random measurement matrix. By applying singular value decomposition (SVD) on the resulting matrix, they found that the singular values increase if there is a target behind the wall; which means that it is possible to detect humans using this method.

Various CS algorithms have been used in TWRI; Table 1.1 summarizes some of the algorithms used. In Section 3.4, a comparison between such algorithms is presented.

Table 1.1: CS Algorithms Used in TWRI Literature

| CS Algorithm | Name | Reference |
|-------------------|---|----------------------|
| OMP | Orthogonal Matching Pursuit | [13, 14, 15, 16, 17] |
| CoSaMP | Compressive Sampling Matching Pursuit | [2] |
| MESI | Multipath Elimination by Sparse Inversion | [18] |
| SpaRSA | Sparse Reconstruction by Separable Approximation | [19] |
| CVX* | CVX: Matlab Software for Disciplined Convex Programming | [20, 21, 22] |
| NESTA | Nesterov's Algorithm | [23] |
| ℓ_1 -magic** | ℓ_1 -magic Recovery of Sparse Signals via Convex Programming | [24, 8, 25] |
| BCS | Bayesian Compressive Sensing | [26] |

* CVX is a Matlab-based modeling system for convex optimization and is not only for CS.

** ℓ_1 -magic is a package that contains a collection of CS algorithms.

1.2.3 Multipath Exploitation

Efforts to exploit multipath signals in TWRI were presented in [27, 28, 29, 30]. In [27], the authors introduced a multipath model for an enclosed room containing four walls, they demonstrated analytically that the multipath ghosts will appear near the wall and its position depends on the sensors locations. They also developed a multipath exploitation technique, depending on their model, to map each multipath ghost to its corresponding target. This helps in reducing the false positives in the image and increasing the signal-to-clutter ratio (SCR) at the true target location. Further improvements on [27] were lately presented in [28]. They used a

householder transformation to express specular reflections. This allows straightforward modelling of multiple reflections for non-rectangular rooms; which were not possible in the model presented in [27]. Using this model, the locations of the ghosts were first estimated assuming free-space, and then used to initialize a non-linear least square optimization formulated to estimate the ghost locations in the through-wall case. Instead of using a spherical weighting to map the multipath ghosts, as done in [27], they used the point spread function (PSF) to directly map the multipath ghosts to their corresponding target positions.

A new attempt to combine multipath exploitation with CS was proposed in [29]. They used two methods; in the first method they assumed equal attenuation in all propagation paths and the targets to be isotropic scatterers. This is then solved with a CS reconstruction method. The second method overcomes the limitation of the first by utilizing group sparsity using a mixed-norm optimization approach. Their simulation results showed a relatively good reconstructed image quality. However, their work, like most of other research on multipath cancelation and exploitation, is built on the assumption of prior knowledge of the scene geometry; which is not always the case in real life applications. An algorithm was recently proposed in [30] for removing multipath in TWRI without requiring prior knowledge about the geometry of the scene. First, they identify the impulse response of the strongest target reflection which is called the primary target. Then they compute a delay operator that matches similar reflections in the residual data to the primary response. Finally, they update the waveform to compensate for any distortions due to the through wall propagation.

1.3 Thesis Contribution

The main aspects that distinguish the work presented in this thesis from previous work in the area are as follows:

1. We introduce the use of F_1 -score in evaluating the performance of CS algorithms. Unlike other performance measures, the F_1 -score gives a quantitative measure of how reliable the algorithm is in terms of detecting the true targets without missing any of them or introducing false targets.
2. We evaluate the performance of fourteen CS algorithms when applied to TWRI. Various factors such as SNR level and compression rate are taken into consideration. To the best of our knowledge, no such comparison has been done in the field.
3. We present a general framework for jointly estimating the interior wall positions of the unknown scene and exploiting the multipath signals resulting from these walls. This will allow for further research in designing effective multipath exploitation algorithms within this general framework.
4. We propose two multipath algorithms within our general framework and test their performance for several scenarios. Successful results of accurate wall position detection and ghost-free images have been obtained.

1.4 Thesis Organization

The remaining part of the thesis is organized as follows: Chapter 2 contains the required technical background. In particular, we give an overview about TWRI systems, the mathematical models used to describe such systems, and the main sources of challenge in TWRI. Also, a summary of two main imaging methods in TWRI is included in this chapter. Chapter 3 then describes the methodology used for evaluating CS algorithms in the context of TWRI. It introduces the notion of F_1 -score, used as a measure, and discusses the results obtained. A general Wall Pursuit (WP) framework for estimating the wall positions and exploiting multipath signals is described in Chapter 4, along with two proposed algorithms within this framework, namely the basic Wall Pursuit (WP) and the Dynamic Wall Pursuit (DWP) algorithms. Simulations results of the implementation of this algorithm are also presented in this chapter. This thesis is concluded in Chapter 5 with a summary of the work and suggestions for future research in the area.

1.5 Notation

The font-types and symbols used throughout the thesis, unless stated otherwise, are briefly described in the following table:

Table 1.2: Notation used throughout the thesis

| Symbol | Description |
|--|--|
| x | Scalars |
| \mathbf{x} | Vectors |
| $x(i)$ | The i^{th} element in a vector \mathbf{x} |
| \mathbf{M} | Matrices |
| $[\mathbf{M}]_{i,j}$ | The element in the i^{th} row and j^{th} column of a matrix \mathbf{M} |
| $\ \mathbf{x}\ _0$ | ℓ_0 "norm": $\ \mathbf{x}\ _0 = \{x(i) \neq 0\} $ |
| $\ \mathbf{x}\ _1$ | ℓ_1 norm: $\ \mathbf{x}\ _1 = \sum_{i=1}^n x(i) $ |
| $\ \mathbf{x}\ _2$ | ℓ_2 norm: $\ \mathbf{x}\ _2 = \sqrt{\sum_{i=1}^n x(i)^2}$ |
| $Blkdiag(\mathbf{M}_1, \mathbf{M}_2, \dots, \mathbf{M}_n)$ | Construct a block diagonal matrix with the matrices $\mathbf{M}_1, \mathbf{M}_2, \dots, \mathbf{M}_n$ being in the diagonal. |
| δ_{ij} | The Kronecker delta, $\delta_{ij} = \begin{cases} 1, & i = j \\ 0, & i \neq j \end{cases}$ |

CHAPTER 2: BACKGROUND

This chapter presents technical background required for this thesis. The signal model for impulse radar based TWRI along with the technique used to detect moving targets, namely CD, are first introduced. Also, major challenges facing TWRI are briefly described. Further, the back-projection and the CS-based imaging techniques are explained.

2.1 Overview

In TWRI, it is necessary to produce high resolution images that accurately describe the scanned region. This requires the use of signals with extremely wide frequency bandwidths. UWB signals are considered to be the perfect candidates since their characteristics fulfil the requirements. Generally, these signals are generated by either transmitting impulse signals or stepped-frequency continuous-wave (SFCW) signals; other methods exist, however these two are the most popular in TWRI [1]. In impulse radar, a short pulse with duration less than a nanosecond is transmitted, thus allowing for high resolution. On the other hand, SFCW radar is based on sequentially transmitting a discrete number of frequencies and observing the response at each frequency; hence acquires the total response in the range of desired

frequencies. In this thesis, our concentration is based on the former technique, though the work done can be easily translated to the latter.

2.2 Through-the-Wall Impulse Radar

In impulse TWRI, the region of interest is scanned by transmitting a short pulse and processing the received reflected signals. The transmitter interrogates the scene by transmitting wideband Gaussian, $s(t)$, pulses given by:

$$s(t) = \frac{1}{\sqrt{2\pi\sigma^2}} e^{-\frac{(t-\mu)^2}{2\sigma^2}}. \quad (2.1)$$

where σ and μ are the standard deviation and the midpoint delay of the Gaussian pulse in seconds, respectively. Assuming M time-multiplexed transmitters and N simultaneous receivers, the signal emitted from the m^{th} transmitter and reflected from a point target q is received at the n^{th} receiver as:

$$y_{mn}(t) = \sigma_q s(t - \tau_{q,mn}), \quad (2.2)$$

where σ_q is the reflectivity of the target, which is assumed to be independent of frequency and aspect angle, $\tau_{q,mn}$ is the time taken by the signal to travel from the m^{th} transmitter to the target and reflect back to the n^{th} receiver. The time delay $\tau_{q,mn}$ is given by:

$$\tau_{q,mn} = \frac{d(t_m, q) + d(r_n, q)}{c} \quad (2.3)$$

where $d(\cdot, \cdot)$ is the Cartesian distance between two points, c is the speed of the electromagnetic wave, and t_m and r_n represent the m^{th} transmitter and the n^{th} receiver, respectively. The received signal is only a scaled and delayed version of the transmitted pulse. Note that wall attenuation and free-space path loss are not considered in equation (2.3) for notational convenience; they can be easily accommodated by using a scalar factor, as in reference [2].

Figure 2.1 illustrates the geometry of a simple TWRI scenario with one point target.

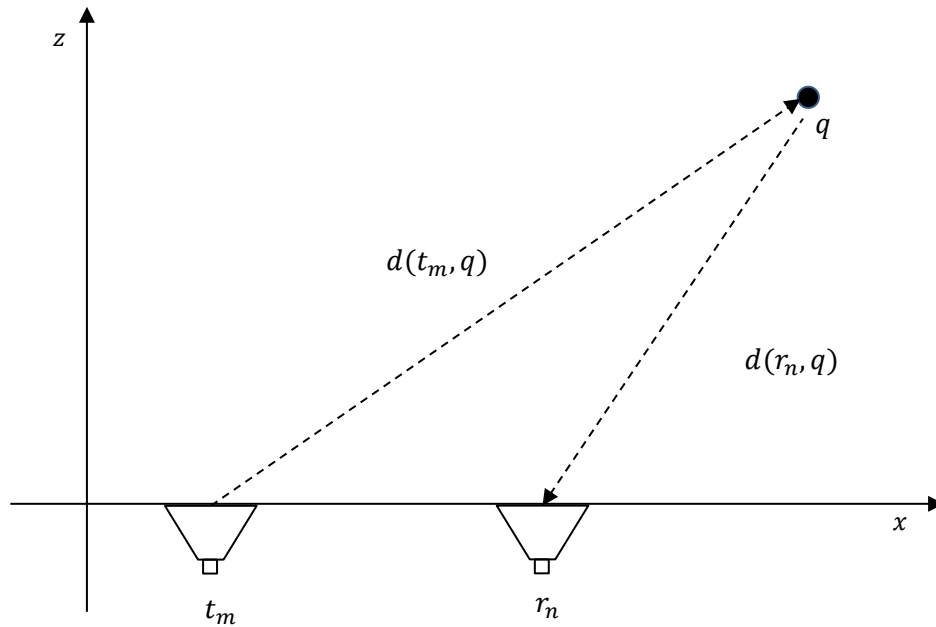


Figure 2.1: Simple geometry of the scene

Under multiple targets scenario, the received signal is the summation of the delayed echoes of the transmitted signal given by:

$$y_{mn}(t) = \sum_{p=1}^P \sigma_p s(t - \tau_{p,mn}), \quad (2.4)$$

where P is the number of targets.

2.3 Moving Objects Indication Using Change Detection

Considering the presence of both stationary and moving objects in the desired scene, equation (2.4) can be expressed as:

$$y_{mn}(t) = \sum_{p_s=1}^{P_s} \sigma_{p_s} s(t - \tau_{p_s, mn}) + \sum_{p_v=1}^{P_v} \sigma_{p_v} s(t - \tau_{p_v, mn}) \quad (2.5)$$

where p_s and p_v represent stationary and moving objects, respectively. Since the returns from stationary objects do not change with time, it is possible to eliminate them by subtracting received signals from two different frames, as follows:

$$\delta y_{mn}(t) = y_{mn}^{(L+1)}(t) - y_{mn}^{(1)}(t) \quad (2.6)$$

where L represents the number of frames between the two received signals. For ease of notation, we deal with each frame as a separate signal. By substituting (2.5) in (2.6) we get:

$$\delta y_{mn}(t) = \sum_{p_v=1}^{P_v} \sigma_{p_v} \left(s(t - \tau_{p_v, mn}^{(L+1)}) - s(t - \tau_{p_v, mn}^{(1)}) \right) \quad (2.7)$$

We will be left with the difference between the returns coming from the moving targets in the two different frames. Here is where the term Change Detection (CD)

comes from; we are detecting the change in the scene reflections which therefore suppresses the stationary returns and enables us to locate moving objects.

2.4 Challenges in TWRI

Accurate imaging of objects behind the wall can be obtained when having single-path propagation between the transmitter and the target without the presence of any obstacles. However, in practical TWRI, signal reflections from the surrounding walls and obstruction from the front wall are inevitable. In the following, we briefly introduce two main sources of challenge, namely the front wall and the multipath reflections.

2.4.1 Front Wall Effect

Effects of the front wall on the received signal include, but are not limited to, signal reflection, refraction, propagation delay uncertainty, and inner wall reverberations. The severity of the effect depends on several wall parameters; related to the wall material and its thickness.

When the electromagnetic waves propagating in the air interact with the material of the wall, they change their direction according to Snell's law:

$$\sin(\varphi_{mq}) = \frac{\sin(\theta_{mq})}{\sqrt{\epsilon_r}}. \quad (2.8)$$

where θ_{mq} and φ_{mq} are the incidence and the refraction angles, respectively. This phenomenon occurs due to change in the transmission medium and is called

refraction, as illustrated in Figure 2.2. If not taken into consideration, the resulting image will mislead the observer by placing the target in a position shifted away from the true one.

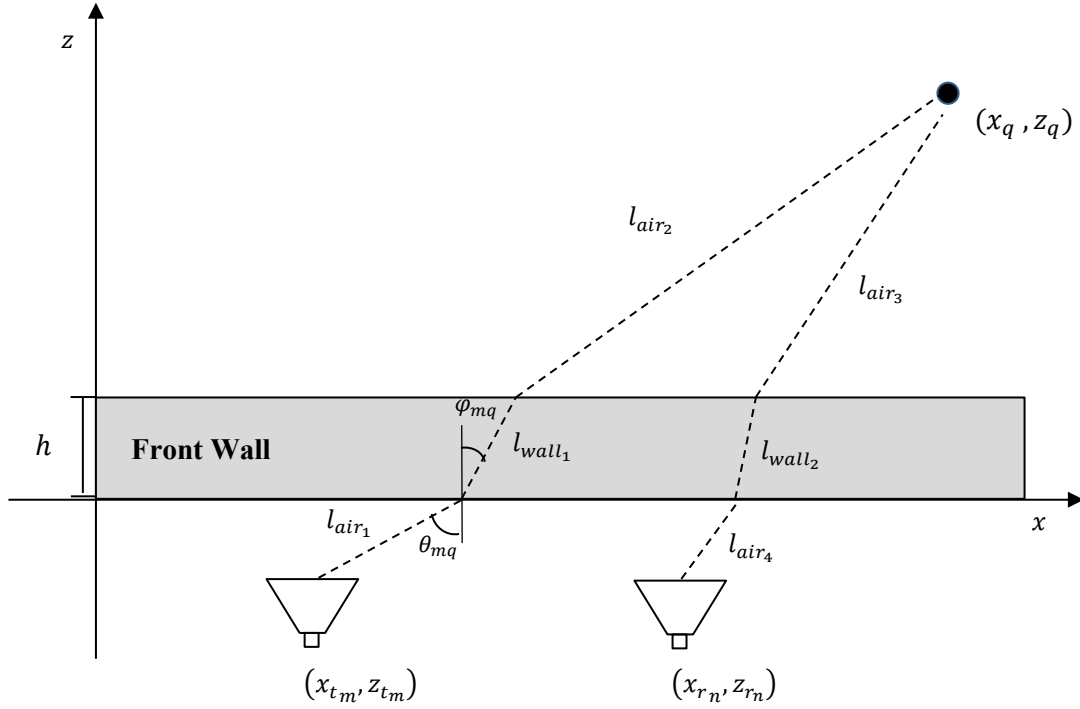


Figure 2.2: Scene geometry in TWRI showing the effect of the front wall.

Another challenge resulting from the front wall is the fact that electromagnetic waves propagation speed decreases when traveling through the wall according to the following relation:

$$v = \frac{c}{\sqrt{\epsilon_r}}$$

where ϵ_r is the relative permittivity of the wall and v is the speed of electromagnetic waves in the wall . Thus the round trip delay of the signal will be:

$$\tau_{q,mn} = \frac{l_{air_1} + l_{air_2} + l_{air_3} + l_{air_4}}{c} + \frac{l_{wall_1} + l_{wall_2}}{v} \quad (2.9)$$

where

$$l_{air_1} = \frac{z_{t_m}}{\cos(\theta_{mq})}, \quad l_{air_2} = \frac{z_q - h}{\cos(\theta_{mq})}, \quad l_{wall_1} = \frac{h}{\cos(\varphi_{mq})}.$$

The same can be computed for the path of the reflected signal. Several approaches have been proposed in the literature to compensate for the front wall ambiguities, as in [31, 32, 33].

2.4.2 Multipath Effect

One of the major challenges in TWRI is multipath stemming from multiple reflections of electromagnetic waves from the target to the walls, floor and ceiling as depicted in Figure 2.3. The signal model in equation (2.4) assumes no multiple scattering effects. It can be modified by adding the multipath reflections as:

$$y_{mn}(t) = \sum_{p=1}^P \sigma_p s(t - \tau_{p,mn}) + \sum_{w=1}^W \sum_{p=1}^P \sigma_{pw} s(t - \tau_{pw,mn}) \quad (2.10)$$

where W is the number of multipath arrivals per target, and $\tau_{pw,mn}$ is the propagation delay of the signal reflecting from target p through path w . When received, the receiver interprets these reflections as real targets and thus *ghost* targets arise in the image.

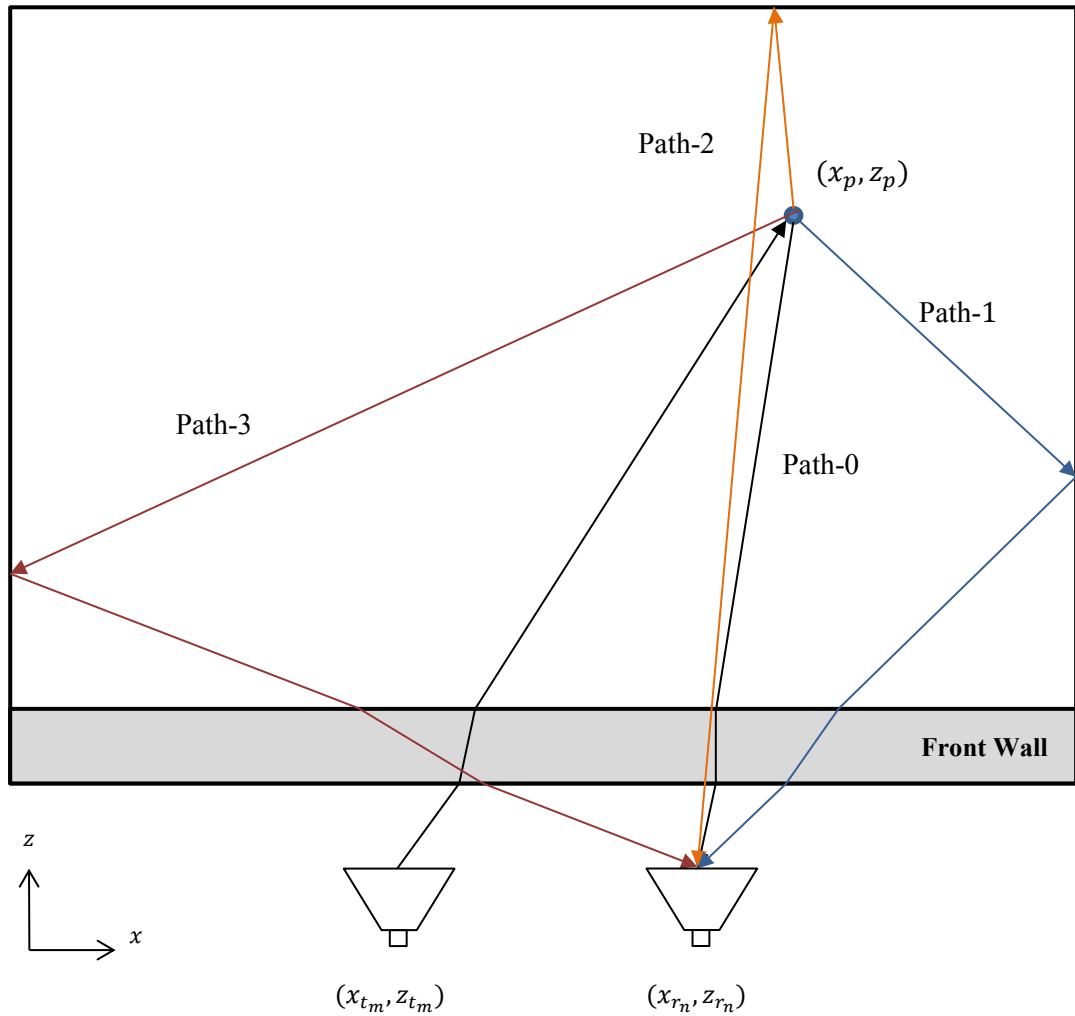


Figure 2.3: The geometry of the scene including the multipath signals

2.5 Imaging Techniques

The main goal of TWRI is to get an image that accurately represents the true scene behind the wall. In the literature, there are a number of methods that accomplish this. In the following subsections, two commonly used imaging techniques are discussed.

2.5.1 Back-Projection

The back-projection method is a simple time-domain approach to get the desired image. The region of interest is first divided into a finite number of small pixels on x and z axis, where x and z represent the crossrange and the downrange, respectively. A signal that represents the contribution of a pixel q located at (x_q, z_q) is obtained by summing delayed versions of the MN received signals, given by:

$$y_q(t) = \sum_{m=1}^M \sum_{n=1}^N y_{mn}(t + \tau_{q,mn}) \quad (2.11)$$

where $\tau_{q,mn}$ is a focusing delay applied to the received signals. Substituting (2.4) in (2.11) yields

$$y_q(t) = \sum_{m=1}^M \sum_{n=1}^N \sum_{p=1}^P \sigma_p s(t - \tau_{p,mn} + \tau_{q,mn}). \quad (2.12)$$

If a target p lies in pixel q , $\tau_{p,mn}$ and $\tau_{q,mn}$ will cancel each other and the signal will be centered back to its original position $s(t)$. The image intensity at pixel q , $I(q)$, is then obtained by applying a matched filter to $y_q(t)$ and sampling at $t = 0$

$$I(q) = y_q(t) * h(t) \Big|_{t=0} \quad (2.13)$$

where $h(t) = s(-t)$ is the matched filter impulse response. This process is repeated for all pixels to get the final image of the scene.

When we apply CD to detect moving targets, equations (2.11), (2.12), and (2.13) are modified by replacing the received signal y_{mn} with the difference signal δy_{mn} to obtain:

$$\delta y_q(t) = \sum_{m=1}^M \sum_{n=1}^N \delta y_{mn}(t + \tau_{q,mn}) \quad (2.14)$$

Substituting (2.7) in (2.14) yields:

$$\delta y_q(t) = \sum_{m=1}^M \sum_{n=1}^N \sum_{p_v=1}^{P_v} \sigma_{p_v} \left(s(t - \tau_{p_v,mn}^{(L+1)}) - s(t - \tau_{p_v,mn}^{(1)}) \right) \quad (2.15)$$

The same imaging process as (2.13) is used to obtain the final image:

$$I(q) = \delta y_q(t) * h(t) \Big|_{t=0} \quad (2.16)$$

2.5.2 CS-Based TWRI

The back-projection imaging method encounters two main problems First, all the received data samples are required to construct the image. Any missing data will lead to deterioration in the image quality, proportional to the amount of missing data. Secondly, in spite of using the whole available data the image is not as

accurate as we desire. To address the above problems, TWRI is implemented under the CS framework.

Consider the following linear system

$$\mathbf{b} = \mathbf{A}\mathbf{x} + \mathbf{v} \quad (2.17)$$

where \mathbf{b} is a $k \times 1$ measured vector, \mathbf{A} is a $k \times N$ known matrix with $k \ll N$, and \mathbf{v} is i.i.d Gaussian noise. CS claims that the signal \mathbf{x} can be perfectly reconstructed with high probability using extremely few measurements than conventional techniques, when certain conditions are met [34, 35, 36]. The first condition is that only few elements of the signal are non-zeros i.e. the signal is sparse in a given domain. The second condition requires the matrix \mathbf{A} to satisfy the restricted isometry property (RIP):

Definition:

For each integer $S = 1, 2, \dots$ define the isometry constant $\delta_S \geq 0$ of a matrix \mathbf{A} as the smallest number such that

$$1 - \delta_S \leq \frac{\|\mathbf{A}\mathbf{x}\|_2^2}{\|\mathbf{x}\|_2^2} \leq 1 + \delta_S \quad (2.18)$$

holds for all S -sparse vectors \mathbf{x} . We say that a matrix \mathbf{A} has the restricted isometry property (RIP) of order S if δ_S is not too close to 1.

If these conditions are satisfied, the sparsest $N \times 1$ vector \mathbf{x} can be reconstructed, with high probability, by solving the following ℓ_1 -minimization problem [37]:

$$\hat{\mathbf{x}} = \min_{\mathbf{x}} \|\mathbf{x}\|_1 \text{ subject to } \|\mathbf{Ax} - \mathbf{y}\|_2 < \epsilon. \quad (2.19)$$

where ϵ is a positive parameter that is related to the noise level. Details of the model used to implement CS in TWRI will be presented in the next chapter, Section 3.2.

CHAPTER 3: EVALUATING COMPRESSIVE SENSING ALGORITHMS IN THROUGH-THE- WALL RADAR VIA F1-SCORE

3.1 Introduction

CS was first introduced to TWRI by Huang *et al.* [7]. Subsequently, a series of research followed in implementing TWRI under CS framework. These include applying CS in detecting human behind the wall [2, 38], mitigating the effect of the front wall [13, 14], determining the interior structure of the building [15], and exploiting the effect of multipath reflections [20, 19, 27, 18, 39].

Various CS Algorithms have been proposed in the literature, however only a limited number of them were applied in TWRI. These include Orthogonal Matching Pursuit (OMP), Compressive Sampling Matching Pursuit (CoSaMP), Sparse Reconstruction by Separable Approximation (SpaRSA) and others. Table 1.1 summarizes the different algorithms used in TWRI literature. Even though these algorithms initially give good results, there is still no concrete argument for which algorithm best suits

TWRI applications. It is desirable to have a specific CS algorithm that utilizes the prior knowledge about the structure of TWRI problems. Several factors should be considered in such algorithm: reconstruction accuracy, processing time, noise immunity and the parameters needed as inputs to the algorithms should be practically available. One example of an impractical parameter for TWRI applications is the number of nonzeros in the image. Having that on mind, it is sensible to first make use of the CS algorithms that have already been devised and evaluate their performance in TWRI applications.

In this chapter, we provide a fairly comprehensive performance investigation of several well-known CS algorithms when applied to TWRI. Since CS algorithms are proliferating, it is impossible to evaluate all of them; for diversity, algorithms with different approaches (greedy, probabilistic, and convex optimization) are considered for evaluation. Table 3.1 provides the list of selected algorithms to be evaluated. Emphasis is given to the effect of different signal-to-noise ratio (SNR) values and compression rates on the reconstructed image quality.

We concentrate on the ability to detect correct targets in the scene reconstructed by the algorithm. Specifically, algorithms producing images which can be correctly classified into targets and non-targets, by setting a threshold, are desired. Thus we adopt the notion of F_1 -score, which is a measure of how precise and sensitive a binary classifier is when comparing its output to the ground truth, to evaluate the performances of the selected algorithms.

This chapter is organized as follows; the formulation of the TWRI problem in the context of CS is detailed in Section 3.2. In Section 3.3, a brief description of the F_1 measure is provided with the procedure for applying it to TWRI. In Section 3.4, an empirical performance comparison between the algorithms when applied to different scenarios of TWRI is provided.

Table 3.1: CS Algorithms Evaluated

| Abbreviation | Name | Reference |
|--------------|---|-----------|
| SpaRSA | Sparse Reconstruction by Separable Approximation | [40] |
| TwIST | Two-Step Iterative Shrinkage/ Thresholding | [41] |
| YALL1 | Your Algorithm for L1 | [42] |
| Fpc_AS | Fixed-Point Continuation Active Set | [43] |
| Fpc | Fixed-Point Continuation | [44] |
| Fpc-bb | Fixed-Point Continuation with Barzilai-Borwein steps | [44] |
| GPSR | Gradient Projection for Sparse Reconstruction | [45] |
| GPSR-bb | Gradient Projection for Sparse Reconstruction with Barzilai-Borwein steps | [45] |
| L1_ls | l_1 -Regularized Least Squares | [46] |
| PCGP | Partial Conjugate Gradient Pursuit | [47] |
| SPGL1-bpdn | Spectral Projected-Gradient for solving BPDN | [48] |
| SPGL1-lasso | Spectral Projected-Gradient for solving LASSO | [48] |
| FL | Bayesian Compressive Sensing Using Laplace Priors | [49] |
| OMP | Orthogonal Matching Pursuit | [50] |

3.2 CS in TWRI

3.2.1 Sparse Reconstruction

Consider the scene with P targets as shown in Figure 3.1. It is desired to form an image of the scene behind a wall of thickness w and dielectric constant ϵ . A UWB MIMO radar system with a set of M transmitters and N receivers is placed at a distance d from the wall and interrogates the scene by transmitting wideband Gaussian pulses given by:

$$s(t) = \frac{1}{\sqrt{2\pi\sigma^2}} e^{-\frac{(t-\mu)^2}{2\sigma^2}}. \quad (3.1)$$

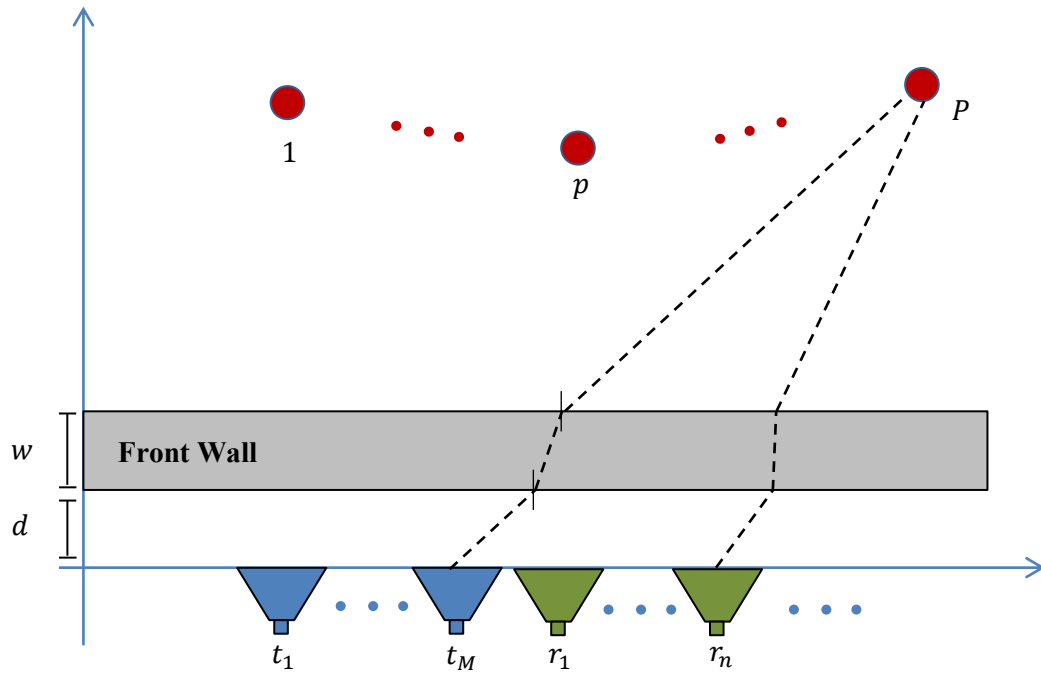


Figure 3.1: Geometry of the scene

where σ and μ are the standard deviation and the midpoint delay of the Gaussian pulse in seconds, respectively. The transmitted signals are assumed to be time multiplexed, while receiving is simultaneous. The signal emitted from the m^{th} transmitter and reflected from P targets is received at the n^{th} receiver as:

$$y_{mn}(t) = \sum_{p=1}^P \sigma_p s(t - \tau_{p,mn}), \quad (2)$$

where σ_p is the reflectivity of the target, which is assumed to be independent of frequency and aspect angle, $\tau_{p,mn}$ is the time taken by the signal to travel from the m^{th} transmitter to the p^{th} target and reflect back to the n^{th} receiver. Note that wall attenuation and free-space path loss are not considered in equation (2) for notational convenience; they can be easily accommodated by using a scalar factor, as in reference [2].

By sampling the received signal $y_{mn}(t)$ at $\{t_k\}_{k=0}^{K-1}$, we obtain a $K \times 1$ column vector, \mathbf{y}_{mn} . The scene is also discretized by dividing it into Q pixels. It is desired to identify which of the pixels contain targets. Following the formulation of [8], we have the linear system of equations

$$\mathbf{y}_{mn} = \mathbf{\Psi}_{mn} \mathbf{r} \quad (3.3)$$

where \mathbf{r} is a $Q \times 1$ vector formed by concatenating the reflectivity values of all the pixels in the scene; the q^{th} element in \mathbf{r} is either equal to zero if there is no target in pixel q , or equal to σ_q if there is a target. The q^{th} column in the $K \times Q$ matrix $\mathbf{\Psi}_{mn}$

contains the signal we expect to receive at the n^{th} receiver if there was a target at pixel q and the signal was transmitted from the m^{th} transmitter. The k^{th} element in the q^{th} column is given by

$$[\Psi_{mn}]_{k,q} = \frac{s(t_k - \tau_{q,mn})}{\|\mathbf{s}_{q,mn}\|_2}. \quad (3.4)$$

$\|\mathbf{s}_{q,mn}\|_2$ is the energy of the signal in the q^{th} column, which implies that each column in Ψ_{mn} has unit norm.

For a typical UWB TWRI application, we are mostly interested in detecting human targets [24]. The majority of UWB TWRI systems have a bandwidth ranged between 500 MHz to 3.5 GHz, which achieves a resolution of 30 to 5 cm [24]. We can assume humans to be roughly equal to point targets in this order of resolution. Since the number of targets in a room is expected to be small compared to its size ($P \ll Q$), \mathbf{r} will be a sparse signal with only P nonzero elements. Therefore, the signal \mathbf{r} can be recovered by applying a sparse reconstruction algorithm that solves the following optimization problem [42], known as the constrained basis pursuit denoising problem

$$\hat{\mathbf{r}} = \min_{\mathbf{r}} \|\mathbf{r}\|_1 \quad \text{subject to } \|\Psi\mathbf{r} - \mathbf{y}\|_2 < \epsilon \quad (3.5)$$

$$\Psi = \begin{bmatrix} \Psi_{11} \\ \Psi_{12} \\ \vdots \\ \Psi_{MN} \end{bmatrix}, \quad \mathbf{y} = \begin{bmatrix} \mathbf{y}_{11} \\ \mathbf{y}_{12} \\ \vdots \\ \mathbf{y}_{MN} \end{bmatrix}$$

where ϵ is a positive parameter, the $MNK \times 1$ vector \mathbf{y} is constructed by vertically concatenating the received signals of all the receivers, and the same is done with the dictionary matrices to get the $MNK \times Q$ matrix Ψ . A variant of (3.5) is the unconstrained basis pursuit denoising problem given by: [42]

$$\hat{\mathbf{r}} = \min_{\mathbf{r}} \frac{1}{2} \|\Psi \mathbf{r} - \mathbf{y}\|_2 + \mu \|\mathbf{r}\|_1 \quad (3.6)$$

where μ is the regularization parameter for the ℓ_1 norm.

3.2.2 Compressing Data Via CS

Directly solving (3.5) might be impractical since large amounts of data need to be stored and processed, thus consuming time and resources [2]. This subsection illustrates how this problem is solved by applying CS in TWRI.

When implementing CS, instead of directly measuring \mathbf{y}_{mn} , its linear projection on a basis Φ_{mn} is measured [38]

$$\tilde{\mathbf{y}}_{mn} = \Phi_{mn} \mathbf{y}_{mn} = \Phi_{mn} \Psi_{mn} \mathbf{r} \quad (3.7)$$

and Φ_{mn} is a $J \times K$ measurement matrix ($J \ll K$). The sparse signal \mathbf{r} can be recovered by solving the following ℓ_1 -norm minimization problem:

$$\hat{\mathbf{r}} = \min_{\mathbf{r}} \|\mathbf{r}\|_1 \quad \text{subject to } \|\Phi \Psi \mathbf{r} - \mathbf{y}\|_2 < \epsilon, \quad (3.8)$$

$$\Phi = \text{Blkdiag}(\Phi_{11}, \Phi_{12}, \dots, \Phi_{MN})$$

To be able to recover \mathbf{r} accurately from (3.8), the matrix Φ_{mn} has to be chosen such that it has minimum mutual coherence with Ψ_{mn} [24]. A matrix Φ_{mn} that has elements that are independent and identically distributed Gaussian or Bernoulli random variables, has been proven to give good results in impulse radar TWRI applications [2].

Many algorithms have been proposed to efficiently solve ℓ_1 norm minimization problems similar to that in (3.8); can be solved using convex optimization, greedy pursuit, or combinatorial algorithms [2]. However, no study has been done to evaluate which of them is practically suitable for TWRI. In section 3.4, an empirical comparison between the performances of different types of algorithms, when applied to TWRI, will be presented.

3.3 Evaluation Criterion

In order to compare different CS algorithms, an evaluation criterion, that takes into account the problem in hand, is needed. The F_1 -score is chosen as the performance measure since it gives a reasonable comparison between different CS algorithms implemented to TWRI. The fundamentals of F_1 -score was laid out in [51], where an information retrieval (IR) effectiveness measure, E , was introduced; E is the complement of the F_1 -score: $E = 1 - F$. F_1 -score has been used as performance measure in information retrieval [51], natural language processing [52], video tracking [53], and radar [54, 55], to name a few.

We would like to correctly classify each pixel in an unknown scene into two categories: targets and non-targets. One mistake that could happen is classifying empty regions as targets, which results in having false alarms (also known as false positives, FP). The opposite could also happen where true targets are classified to be non-targets, resulting in having missed targets (also known as false negatives, FN). The correctly classified regions are called true positives, TP , and true negatives, TN , for correctly classifying targets and non-targets, respectively. If the true target is actually represented with a group of pixels, we define a TP to be the detection of any one of these pixels, and a FN to be the failure of detecting any of these pixels.

The accuracy of a classifier depends on the ratio between the number of targets correctly detected and all the detected targets, known as precision, and the ratio between the number of targets correctly detected and all the true targets, known as recall.

$$\text{precision} = \frac{TP}{TP + FP} \quad (3.9)$$

$$\text{recall} = \frac{TP}{TP + FN} \quad (3.10)$$

Since precision and recall are both necessary for evaluating the detection capabilities of an algorithm, it is convenient to find a single measure that considers both of them. One measure that combines both of them is the F_1 -score, which is the harmonic mean of the precision and recall

$$\begin{aligned}
F_1 &= 2 \cdot \frac{\text{Precision} \cdot \text{Recall}}{\text{Precision} + \text{Recall}} \\
&= \frac{2 \cdot TP}{2 \cdot TP + FN + FP}.
\end{aligned}
\tag{3.11}$$

Taking the harmonic mean is more reasonable than taking the arithmetic mean. For example, if a classifier has recall = 1 and precision = 0.4, this means that it detects all the true targets but has many false alarms, thus its performance is bad. In such a case, the arithmetic mean is 0.7, however the harmonic mean, F_1 -score, is 0.29, which reflects the bad performance of the classifier.

In the next section, the F_1 -score is used to test the performance of different CS algorithms when applied to TWRI. However, CS algorithms return continuous values for each pixel rather than a binary classification of target or non-target. This continuous value can be turned into a binary classifier by setting a threshold η and classifying pixels with values greater than η as targets and those less than η as non-targets. Two hypotheses are formed for each pixel

$$\mathcal{H}_0: \text{no target in pixel } p, \quad \text{if } r(p) < \eta$$

$$\mathcal{H}_1: \text{a target in pixel } p, \quad \text{if } r(p) > \eta.$$

The resulting output of an algorithm is first normalized to give values between 0 and 1. Then a threshold is chosen in order to get a binary classification of the scene (target or non-target). The threshold is adjusted such that it results in the maximum

F_1 -score that the given algorithm can achieve. This maximum value represents the performance of the algorithm

$$F_{CS} = \max_{\eta} F_I(\eta). \quad (3.12)$$

Accordingly, we are looking for the best F_1 -score that the algorithm can achieve, regardless of the considered value of η . If $F_{CS} = 1$, it means that the algorithm is able to retrieve all the true targets without any misclassifications, if η is chosen properly. On the other hand, if $F_{CS} < 1$, the algorithm will always result in misclassifications.

3.4 Results and Discussion

In order to compare different CS algorithms in TWRI applications, several numerical examples are presented in this section. The simulated scene is a $4 \text{ m} \times 4 \text{ m}$ region behind a 20 cm thick wall with a dielectric constant $\epsilon_r = 6$. For simplicity, the effect of the front wall on the received signal is assumed to be taken care of using the available methods [6,7]. Three transmitters are placed 0.8 m away from the front wall with 0.9 m interspacing between them. The antenna in the center is also used as a receiver. A Gaussian pulse of width 0.7 ns is used to interrogate the scene. The time step used in simulation is $\Delta t = 50 \text{ ps}$ and the total number of time steps is $K = 800$.

Four random targets of size $25 \text{ cm} \times 25 \text{ cm}$ were generated and the CS algorithms, listed in Table 3.1, were used to reconstruct the image. Since we are measuring the

practicality of the algorithms, the processing time of the algorithm should be reasonably small to allow for real-time imaging. Thus, to make a fair comparison, the algorithms were allowed to work for a limited time slot of 0.2 seconds. The performance of each CS algorithm was then measured by taking the F_1 -score after averaging the precision and recall over 100 runs. We concentrated on the effect of varying SNR, and size of the measurement matrix Φ on the performance of a given algorithm.

Each CS algorithm has some parameter that should be set in order to get the algorithm working properly. If chosen improperly, it could decrease the performance of the algorithm. To have a fair comparison between the algorithms, similar regularization parameters, have been used.

3.4.1 Detection Performance vs. SNR

Figure 3.2 shows the performance of the algorithms under different SNR values, when all the data is used and only 10% of the data. It can be observed that some of the algorithms that perform well in high SNR might not be the best choice when having low SNR. It is noted that the performance of some CS algorithms is a strong function of the SNR. Thus, to achieve acceptable performance in our system, algorithms which are mostly invariant to SNR values are desired. It is found that YALL1 has the best performance in low SNR values, whereas SPGL1-lasso and L1-ls have the worst when reduction is applied. The other algorithms have similar moderate performance. In practical TWRI, we need to process a highly cluttered noisy signal with low SNR.

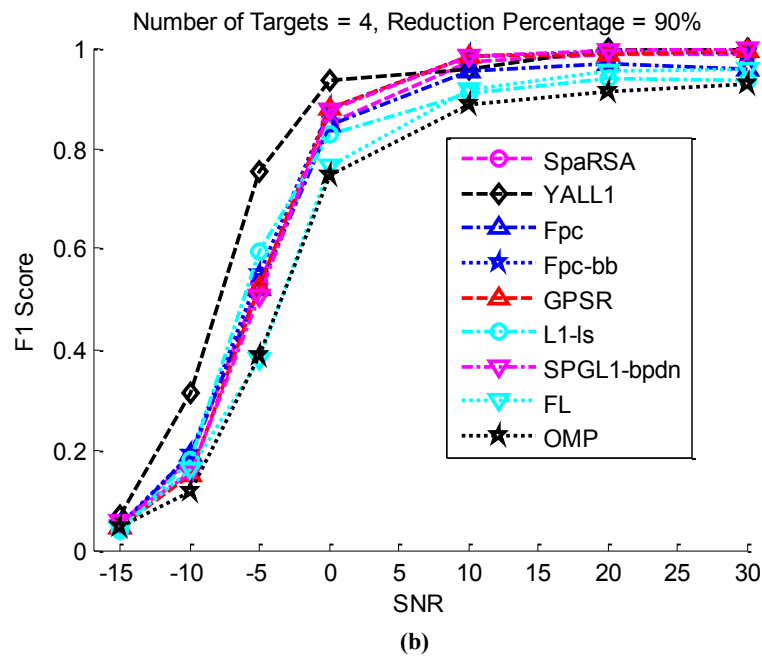
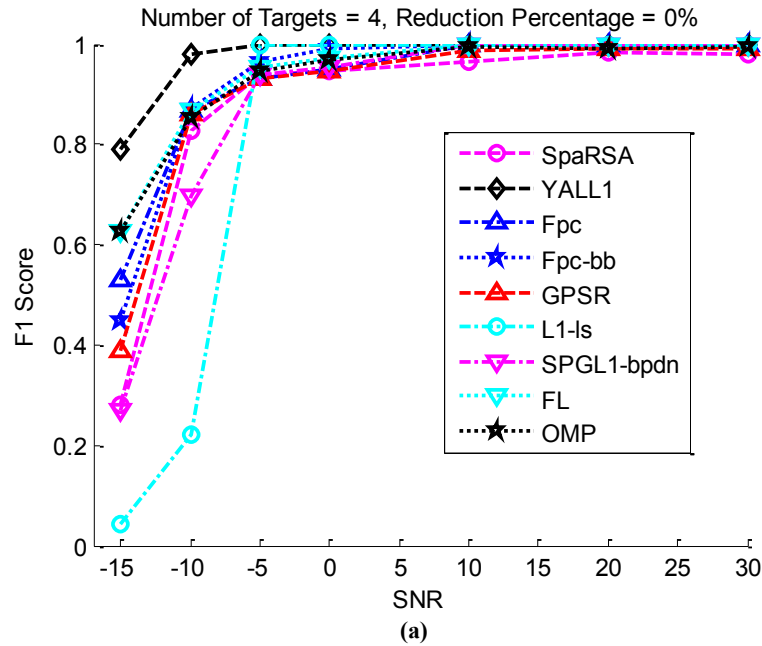


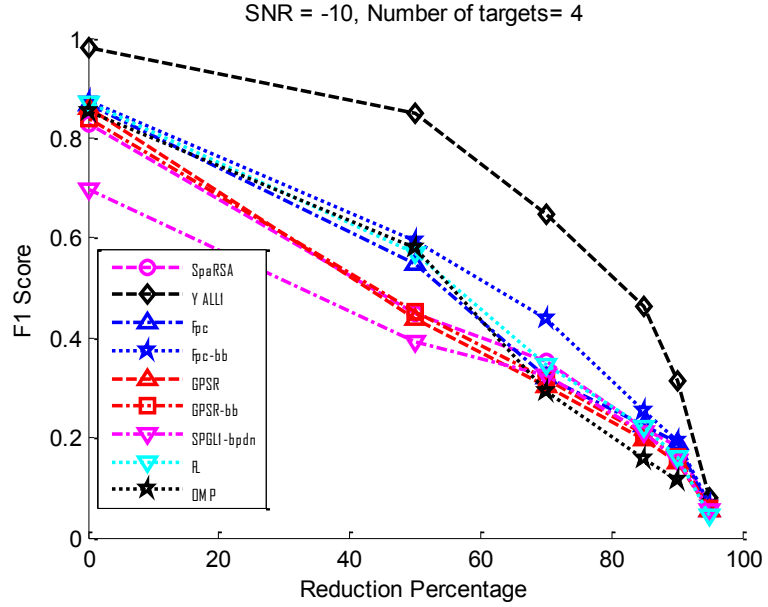
Figure 3.2: Performance of CS algorithms when varying the SNR, (a) all the data is used, (b) 10% of the data is used (for clarity, only the 9 algorithms are shown)

3.4.2 Detection Performance vs. Compression Rate

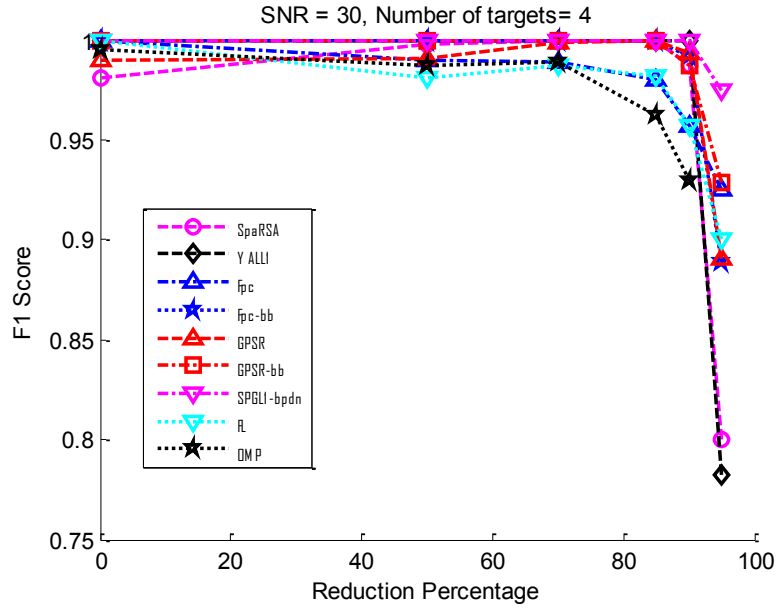
The performance of the algorithms under different reduction percentages, with SNR = -10 and 30, is shown in Figure 3.3. For low SNR values, the detection

capabilities of the algorithms decrease rapidly with increased reduction. YALL1 seems to be the best in this case, where it still gives reasonable results when having up to 50% percent reduction. On the other hand, for high SNR values, most of the algorithms are not highly affected when the percentage of reduction is increased; meaning that similar performance can be obtained with fewer amounts of data. It is found that the following algorithms perform well in high reduction percentages: GPSR-bb, SPGL1-bpdn, Fpc-bb, YALL1 and SpaRSA. However when the percentage of reduction exceeds 90%, the performance of the two latter algorithms decreases.

It can also be observed that the performance of some algorithms, such as SpaRSA, increases when Φ is reduced until it reaches a point where it decreases afterwards. This is because reducing the size of the matrix Φ has two main effects on the algorithm. First, it decreases the amount of computations and hence processing needed for a single iteration. On the other hand, this reduction makes the system more underdetermined, thus increasing the number of iterations needed to get acceptable results. Reducing the size of Φ not only reduces processing time but also hardware complexity, such as having less memory and less arithmetic operations.



(a)



(b)

Figure 3.3: Performance of CS algorithms when varying the size of the measurement matrix, SNR = (a) - 10 dB, (b) 30 dB (for clarity, only the 9 algorithms with best performances are shown)

3.4.3 Regions of desired performance

To be able to see the effect of both SNR and the compression rate, a graph showing the effect of these two factors on the algorithms performance is shown in Figure 3.4. The curve represents the contour where an algorithm achieves a performance of $F_1 = 0.9$. Above this curve is the region where the algorithms performance is $F_1 \geq 0.9$, meaning that if there are five truly detected targets we can withstand having either one *FN* or one *FP* at maximum. This graph helps in identifying the algorithm with the best performance, for a given SNR, and the percentage of compression that achieves that. It is observed that YALL1 spans the widest region with the desired performance followed by SpaRSA, FPC, and GPSR-bb with similar performance regions.

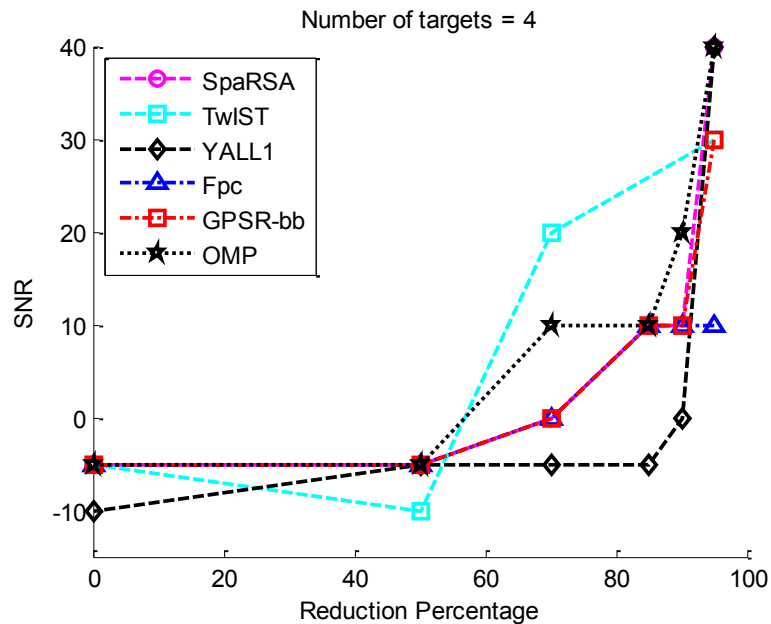


Figure 3.4: Algorithms region of desired performance ($F_1 \geq 0.9$) (for image convenience, only the 6 algorithms with best performances are shown)

3.5 Conclusion

TWRI faces significant challenges; of which is the large amount of data that need to be saved and processed. CS allows for signal reconstruction using very few measurements. Many algorithms exist in literature for solving CS problems; however they have not been comparatively evaluated when applied to TWRI. In this chapter, the performances of the most popular CS algorithms were compared, by means of maximum F_1 -score, when applied to TWRI.

For high values of SNR, all the algorithms perform well when the reduction rate is small. When the reduction rate is increased, FPC-AS works poorly, YALL1 and SpaRSA perform moderately, and the remaining algorithms have similar good performance. For low SNR, YALL1 has the best performance for all reduction percentages, and SPGL1-lasso and L1-ls have the worst compared to the others.

CHAPTER 4: JOINT WALL POSITION DETECTION AND MULTIPATH EXPLOITATION IN TWRI

4.1 Introduction

In this chapter we introduce a general framework for jointly recovering the room geometry and a ghost-free image of the scene. Two algorithms are proposed within this framework. The first algorithm utilizes the fact that when false wall positions are considered, the reconstructed image will be populated with false targets. The algorithm starts by finding one wall position, in each considered direction, that minimizes the number of targets in the scene. When that it is found, the dictionary is updated with the multipath returns of the detected walls and is used in a subsequent search, with the same goal of minimizing the number of targets in the scene. This process is repeated until a stopping criterion is reached. The second algorithm builds on the first one and extends it to make use of moving targets in the scene. Results show the effectiveness of the first algorithm in high SNR values. They also

show that moving targets increase our knowledge of the wall positions. When this is utilized, as in the second algorithm, accurate wall position detection is obtained even in low SNR values

The remainder of this chapter is organized as follows. Section 4.2 presents the multipath model used in this research. A general framework for detecting the interior wall positions is introduced in Section 4.3. An algorithm within this framework is then proposed in Section 4.4. This algorithm is further extended in Section 4.5 to include moving targets. Finally we summarize and conclude in Section 4.6.

4.2 Multipath Model

One of the major challenges in TWRI is multipath stemming from multiple reflections of EM waves from the target to the walls, floor, and ceiling. The receiver interprets these multipath signals as reflections from physical targets and considers them as real targets; these hypothetical targets are called ghost targets. The received signal with multipath can be expressed as:

$$\tilde{\mathbf{y}} = \mathbf{\Psi}^{(0)} \mathbf{x}^{(0)} + \mathbf{\Psi}^{(1)}(\mathbf{w}_1) \mathbf{x}^{(1)} + \dots + \mathbf{\Psi}^{(R)}(\mathbf{w}_R) \mathbf{x}^{(R)}, \quad (4.1)$$

where the first term corresponds to the direct path while the others correspond to multipath coming from R different paths. The wall positions are discretized and each element in \mathbf{w}_r represents a wall position in direction r , $r = 1, 2, \dots, R$. In the case that only one back-wall and two side-walls are present, $R = 3$. This vector will have

at most one nonzero element, with a value of 1, corresponding to the position of the wall in direction r . The dimension of \mathbf{w}_r is proportional to the resolution of discretization and the wall range considered. The dictionary matrix $\Psi^{(r)}(\mathbf{w}_r)$ contains the returns of the r^{th} path, and $\mathbf{x}^{(r)}$ is a vector that contains the corresponding target reflection coefficients for that path.

Equation (4.1) can be rewritten in a compact form as

$$\tilde{\mathbf{y}} = \tilde{\Psi}(\mathbf{w})\tilde{\mathbf{x}} \quad (4.2)$$

where

$$\begin{aligned} \mathbf{w} &= [\mathbf{w}_1^T \quad \mathbf{w}_2^T \quad \dots \quad \mathbf{w}_R^T]^T, \\ \tilde{\Psi} &= [\Psi^{(0)}, \quad \Psi^{(1)}(\mathbf{w}_1), \quad \dots, \quad \Psi^{(R)}(\mathbf{w}_R)], \\ \tilde{\mathbf{x}} &= [\mathbf{x}^{(0)T}, \quad \mathbf{x}^{(1)T}, \quad \dots, \quad \mathbf{x}^{(R)T}]^T. \end{aligned}$$

This formulation is similar to that provided in [56], except that \mathbf{w} in our case is a vector.

If the scene is reconstructed by using only the direct path returns, multipath signals will be thought to be reflections of real targets and thus ghost targets will appear in the image. On the other hand, if the wall positions are known, \mathbf{w} is known, it is possible to construct the dictionary matrix $\tilde{\Psi}(\mathbf{w})$ and reconstruct a ghost free image by applying the following optimization problem

$$\min_{\tilde{\mathbf{x}}} \|\tilde{\mathbf{x}}\|_{1,2} + \lambda \|\tilde{\mathbf{y}} - \tilde{\Psi}(\mathbf{w})\tilde{\mathbf{x}}\|_2 \quad (4.3)$$

where

$$\|\tilde{\mathbf{x}}\|_{1,2} = \sum_{q=1}^Q \|[x^{(1)}(q), x^{(2)}(q), \dots, x^{(R)}(q)]^T\|_2.$$

Consequently only real targets will be present in the reconstructed scene.

However, when incorrect wall positions are used to construct the dictionary, wrong multipath propagation delays will be associated with each pixel, thus creating ghost targets in the reconstructed scene.

In the next section an effective reconstruction technique, that jointly estimates the true wall positions and reconstructs a ghost-free image of the scene, is proposed.

4.3 In Pursuit of the Wall Positions

4.3.1 General Framework

Since the true wall positions are unknown, we need to ensure a good estimate of them in order to get a ghost-free image. We exploit the fact that a wrong estimate of the wall positions will lead to a populated scene. In other words, it is desired to find the wall positions that minimizes the number of targets in the scene, and at the same time obeys (4.2). This can be translated to the following mathematical optimization expression

$$\begin{aligned} \hat{\mathbf{w}}, \hat{\mathbf{x}} = \underset{\mathbf{w}, \tilde{\mathbf{x}}}{\operatorname{argmin}} \quad & \|\tilde{\mathbf{x}}\|_{1,2} + \lambda \|\tilde{\mathbf{y}} - \tilde{\Psi}(\mathbf{w})\tilde{\mathbf{x}}\|_2 \\ \text{s.t. ,} \quad & \|\mathbf{w}_r\|_0 \leq 1, \quad \forall r = 1, 2, \dots, R. \end{aligned} \quad (4.4)$$

The solution of (4.4) will give us the wall positions, constrained to the presence of one wall or none in each direction, and the ghost free image. Several methods can be proposed to solve (4.4). One approach is exhaustively searching all possible wall combinations, updating the matrix $\tilde{\Psi}$ each time, and then seeing which results in the sparsest image. This approach is costly and time consuming since we have to search through $\mathcal{O}(R^W)$ different wall combinations.

A simpler approach is to iteratively build the room geometry. That is to first **scan** for the most effective wall positions in each direction separately. These walls are then fixed and the dictionary is updated with the new wall positions. Further, we can refine by repeating this process; we define the number of refinement iterations as the **depth** of the algorithm. The wall positions will converge to the true positions after a couple of refinement iterations and the final image is then obtained using the refined dictionary.

Figure 4.1 is provided to further illustrate this process. First, initial wall positions are given to the multipath dictionary generator (MDG), which generates the initial dictionary $\tilde{\Psi}_0(\mathbf{w})$. For each wall direction, the scanning process starts looking for the most probable wall position in that direction, this step is shown within the dashed boxes in Figure 4.1. Each dashed box is called a **layer** and represents one of the wall directions, thus we have W of them (only 3 are shown in the figure for

visual clarity). The layer on the top is for the r^{th} wall direction. Using $\tilde{\mathbf{y}}$, $\tilde{\Psi}_r(\mathbf{w})$ and $\Psi^{(r)}(\mathbf{w}_r)$, an image $\mathbf{x}_w^{(r)}$ is constructed for the w^{th} wall position and is given a cost $s_r(w)$. This is done for all $w = 1, 2, \dots, W$. The cost function of each wall position, \mathbf{s}_r , is then passed to the MDG, which in turn updates the dictionary and routes it back to the layers if more depth is desired. This process is repeated until all wall positions converge or a specific depth D is reached.

The number of search combinations needed in this method is reduced to $\mathcal{O}(DWR)$, which is far less than that of the exhaustive search method. To illustrate this assume that we are searching in three wall directions, $W = 3$, and for each wall we have twenty hypotheses, $R = 20$. The exhaustive method searches through $(20)^3 = 8000$ possible wall combinations, while the latter method only searches through $D \times 20 \times 3 = 60D$ wall combinations. The depth D needed for convergence will be shown to be a small number.

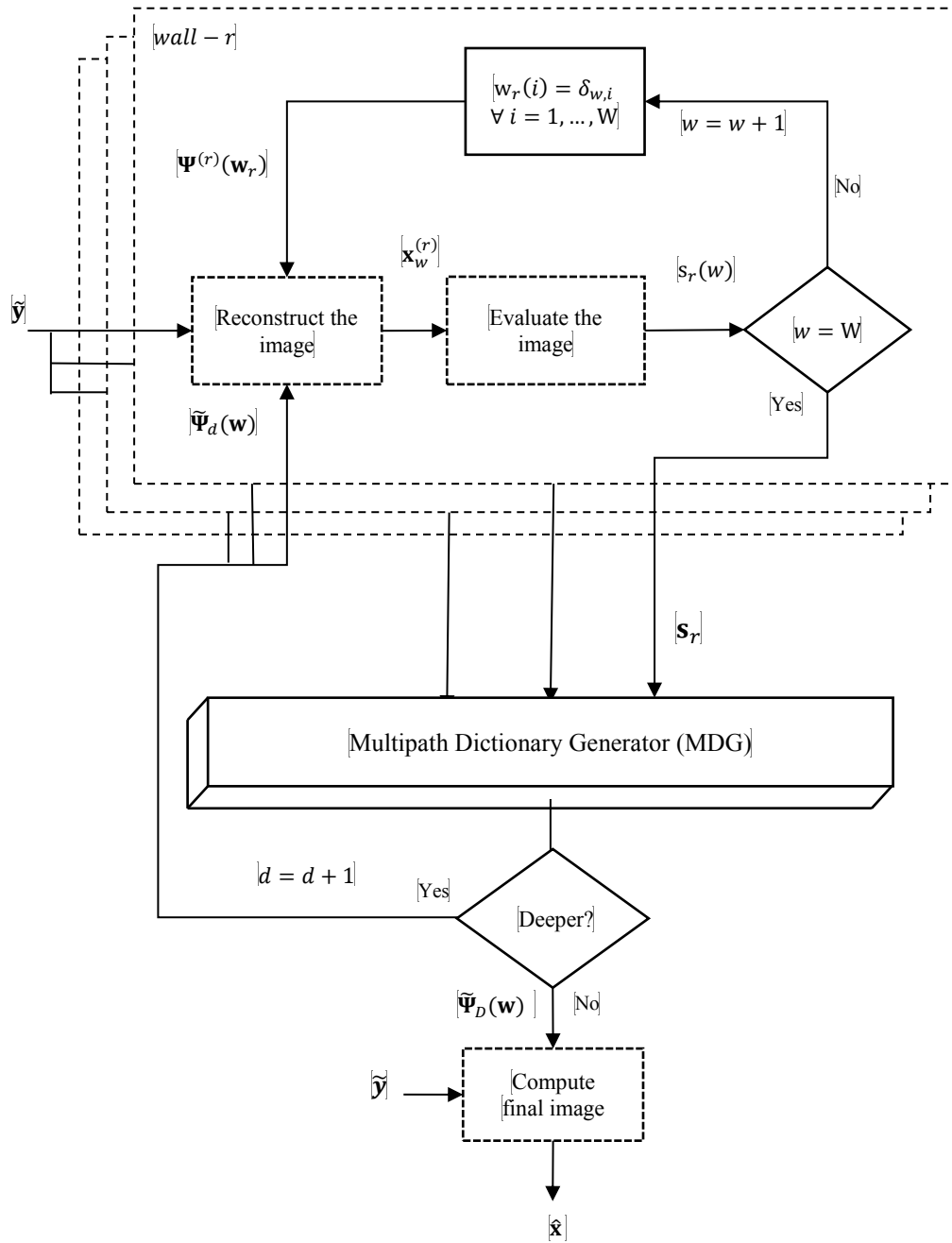


Figure 4.1: The block diagram of the Wall Pursuit general framework.

4.3.2 Variations in the Proposed Wall Pursuit (WP) Framework

In the framework described in the previous subsection, the details of the following steps were intentionally left unspecified:

- 1) **Reconstructing the Image:** This step is performed in each layer. Detecting the correct wall positions strongly depends on this step, thus an imaging method that allows for a clear distinction between wrong wall choices and correct ones should be preferred.
- 2) **Evaluating the image:** This step is also performed at each layer after reconstructing the image. Here, we are looking for a cost function that changes with wall position accuracy such that it increases with images formed from incorrect wall positions and decreases when the wall positions are correct.
- 3) **Updating the dictionary:** From each layer, the MDG receives the expected wall position and its confidence factor. With the aid of these two values, soft decisions on the wall positions, as well as hard ones, can be made.
- 4) **Computing the final image:** The imaging method chosen in this step need not be the same as that chosen inside the layers. Since this is only executed once at the end, it should give accurate results.

These four variations allow for the foundation of a family of algorithms under the general framework. One of these family members will be introduced in the following subsection.

4.4 Basic WP Algorithm

Within the WP framework, we propose an algorithm that detects the true wall positions and reconstructs a ghost-free image. Details of the algorithm along with results discussion are presented in this section.

4.4.1 Variations clarified

Within the WP framework, we propose an algorithm that implements the following with the previously described variations:

- 1) **Reconstructing the Image:** The image $\mathbf{x}_w^{(r)}$ in each layer is reconstructed by solving

$$\mathbf{x}_w^{(r)} = \min_{\tilde{\mathbf{x}}} \|\tilde{\mathbf{x}}\|_{1,2} + \lambda \|\tilde{\mathbf{y}} - \tilde{\Psi}_d(\mathbf{w})\tilde{\mathbf{x}}\|_2 . \quad (4.5)$$

From all the scanned W positions, the correct image should be distinct from the others in terms of sparseness.

- 2) **Evaluating the image:** Since our imaging method distinguishes correct wall positions based on sparsity of the reconstructed image, a reasonable cost function is the mixed $\ell_{1,2}$ norm:

$$s_r(w) = \|\mathbf{x}_w^{(r)}\|_{1,2} .$$

- 3) **Updating the dictionary:** A simple updating criteria is used, where the minimum value of the cost function for each wall is found:

$$s_r(w_{min}) < s_r(w), \quad \forall w = 1, 2, \dots, W,$$

and then \mathbf{w}_r is updated as follows

$$w_r(i) = \delta_{w_{min}, i}, \quad \forall i = 1, \dots, W$$

- 4) **Computing the final image:** The final image is reconstructed using (4.5) with $d = D$. If the algorithm correctly identifies the wall positions, this should result in the best possible image.

4.4.2 Results and Discussion

The following simulated scene was used to test the performance of our method. Three transceivers are placed 1 m away from the front wall with 0.25 m interspacing between them. A 3 m \times 2.5 m image, with a pixel discretization of 5 cm along both downrange and crossrange, of the scene behind a 20 cm thick wall is interrogated using a Gaussian pulse of width 0.73 ns. The time step used in simulation is $\Delta t = 25$ ps and the total number of time steps is $K = 1085$. The effect of the front wall on signal propagation is assumed to be compensated for. Behind the wall lie four point-targets, with perfect reflection, in a 2.6 m \times 2 m room. The received signal contains multipath reflections resulting from the back and side walls, with amplitudes less than that of the direct reflections because of multiple reflections. Additive white Gaussian noise is added to the received signal. A measurement matrix of random equiprobable ± 1 elements, similar to that in [8], performs 20% compression in the acquisition stage.

The effect of the SNR on the algorithm is investigated. Precisely, we would like to see how often the algorithm will give us misleading information about the wall

geometry in the room, as a function of SNR. Also, for the cases where correct wall position results are obtained, we would like to see how deep the algorithm needs to dive to achieve these results. Figure 4.2 gives proper insight for this regard, each curve in Figure 4.2 (a) gives information about the chance of detecting the specified number of walls under the corresponding value of SNR. It can be seen that the algorithm perfectly constructs the correct wall positions in the case of high SNR. When the value of the SNR decreases, a subset of the walls can still be detected however the chances of detecting all the walls decreases. The algorithm will also be more susceptible to being trapped in oscillations. This means that at some depth level d the MDG decides on wall positions that were already visited in previous depth levels. Thus the algorithm will oscillate through the same sequence of wall positions over and over. Figure 4.2 (b) shows the percentage of correctly detecting the three walls, detecting only a subset of the walls, and oscillations. Another interesting observation from Figure 4.3 is that when we are four levels deep in the algorithm at least two walls have been successfully detected for the given range of SNR.

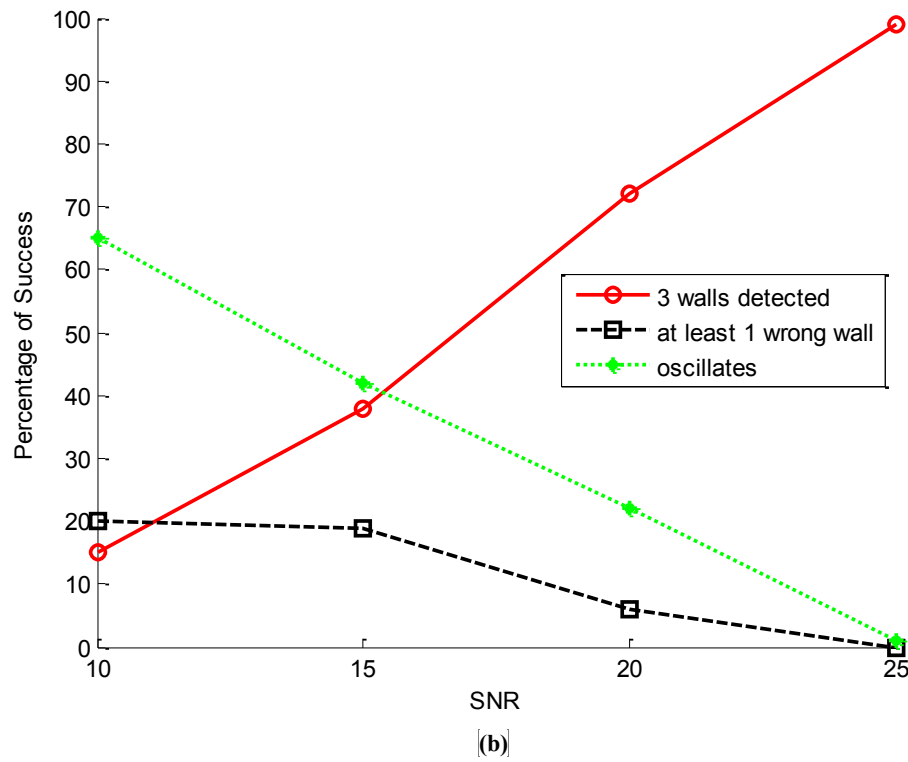
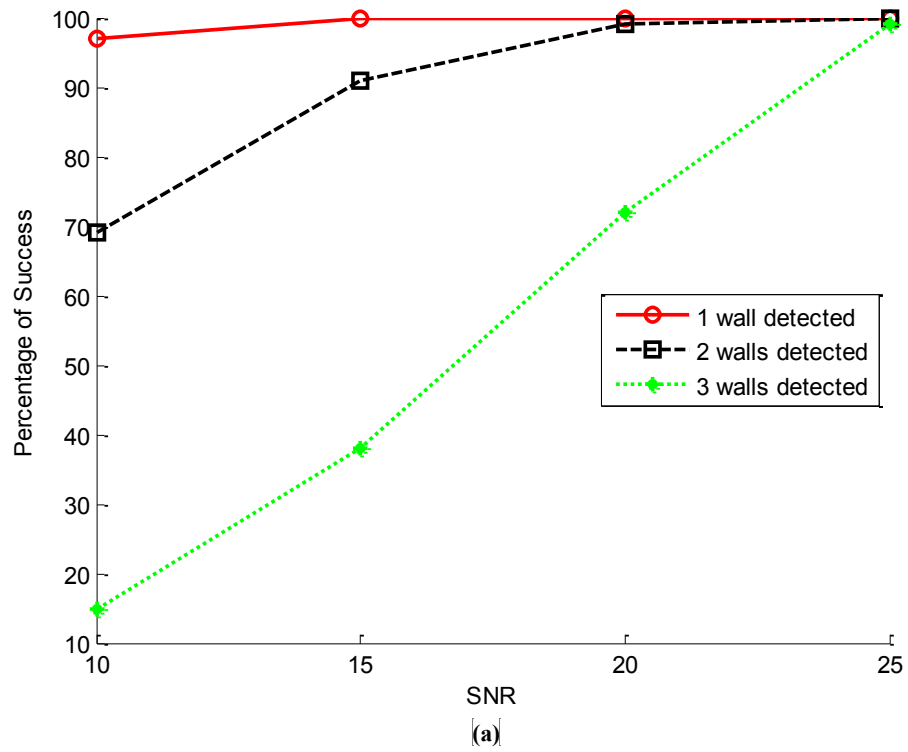


Figure 4.2: (a) Percentage of successfully detecting the walls with variation in SNR (dB), (b) The status of the algorithm at the end for each SNR.

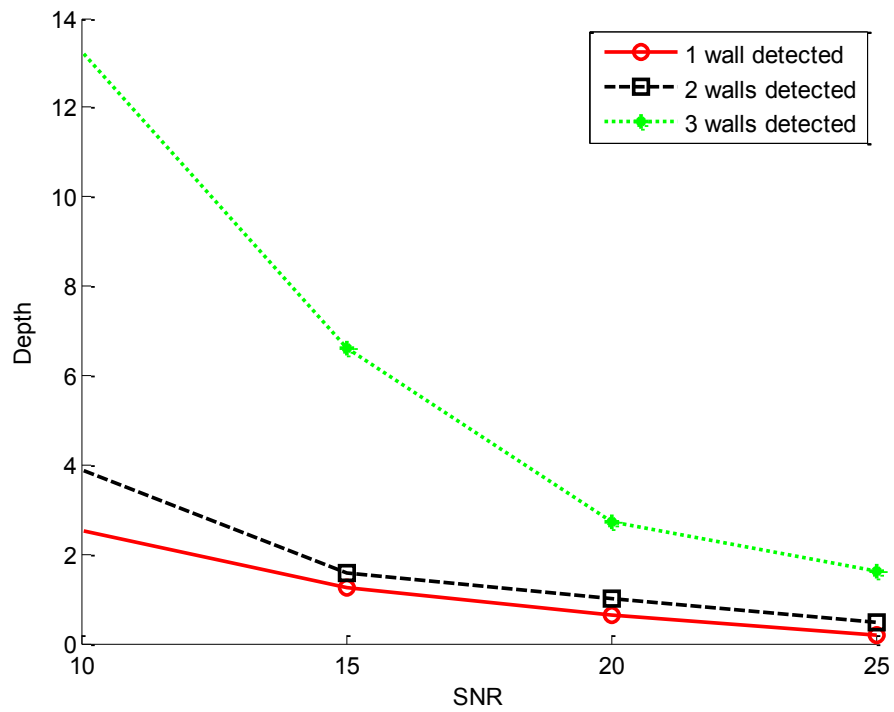


Figure 4.3: The average level of depth needed to achieve the success rate given in Figure 4.2 (a).

4.5 Dynamic Wall Pursuit (DWP) Algorithm

The previous algorithm is described for a received signal in a given snapshot of the scene. To be able to continuously get a ghost-free image, one option is to process the received signal in first snapshot until the final updated dictionary $\tilde{\Psi}_D(\mathbf{w})$ is obtained. This dictionary is then used to reconstruct later images. The drawbacks of this approach is that it might take a long time to converge, its performance decreases in low SNR, and it does not make use of the dynamic information we get from moving targets in the scene. This section presents the Dynamic Wall Pursuit (DWP) algorithm, which is an extension of the WP algorithm that allows it to make use of the dynamic property of the problem to improve wall detection performance.

4.5.1 Extensions to WP

In many applications of TWRI, the target of interest is moving, thus the received signal is changing. This can be utilized to further improve the accuracy of wall detection. The presence of a moving target inside the room means that more information about the wall positions is gained with time. Three simple, but effective, extensions are made:

- 1) CD is used to detect moving targets and suppress returns from stationary objects. This helps in increasing the sparsity of the scene, thus improving the performance of the CS algorithm used to reconstruct the images.

- 2) The MPG accumulates the cost of each wall, $s_r(w)$, from different time frames. Thus, information from earlier frames will still have an influence on the MPG's choice of wall updates.
- 3) For each frame, the WP algorithm is applied until a specific depth D is reached. The value of D is chosen such that at least one or two walls are detected. We have seen that in most cases when D is from two to four, we are able to detect two walls for SNR above 10 dB .

4.5.2 Results and Discussion:

The same setup of the previous simulation is adopted to test the performance of the DWP. Four moving point targets of speed ranging between 0.5 to 1.5 m/s are simulated to move inside the room; the speed of a human walking or suddenly changing direction is within this range [57]. Since the resolution of the image is taken to be 5 cm , a frame rate of 10 frames per second will be convenient. The algorithm is processed for only 35 frames and then evaluated. In each frame, a depth level of $D = 2$ is chosen. The results in this section are averaged over 100 runs. In each run, initial target location, target moving path, and speed are all chosen uniformly random.

We would like to see the performance of this algorithm when varying SNR values. Also, for the cases where correct wall positions are obtained, we would like to see how many frames are needed to get accurate information about the room geometry.

Figure 4.4 shows that DWP algorithm is successful in detecting all the walls when the SNR is above 15 dB, and at least two walls when it is below that. Compared to WP, DWP results in improved wall detection and hence a better image of the scene, as shown in Figure 4.4. When DWP succeeds in detecting all the walls, it does so in a significantly fast manner. Figure 4.5 and Figure 4.6 show the average number of frames and the histogram of the frames needed to find the correct wall positions, respectively. When the SNR is 15 dB, the algorithm successfully detects the walls on an average of 6 frames, and 25 frames on maximum as shown in Figure 4.5 and Figure 4.6 respectively.

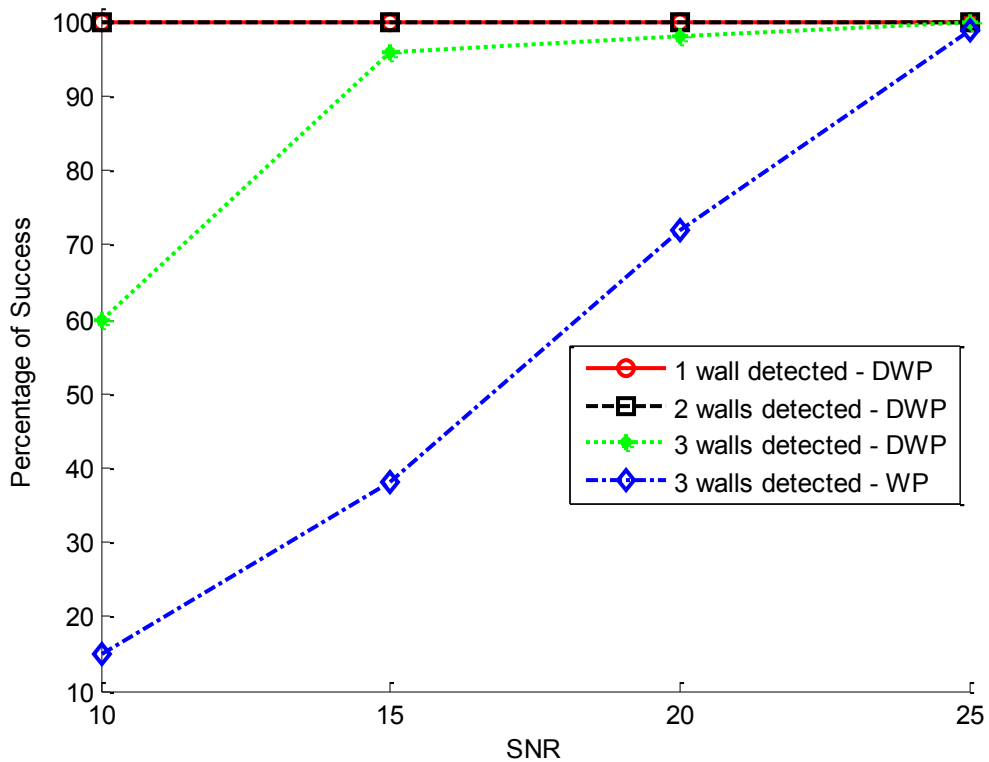


Figure 4.4: A comparison between the two proposed algorithms with respect to the percentage of successfully detected walls, with variation in SNR (dB).

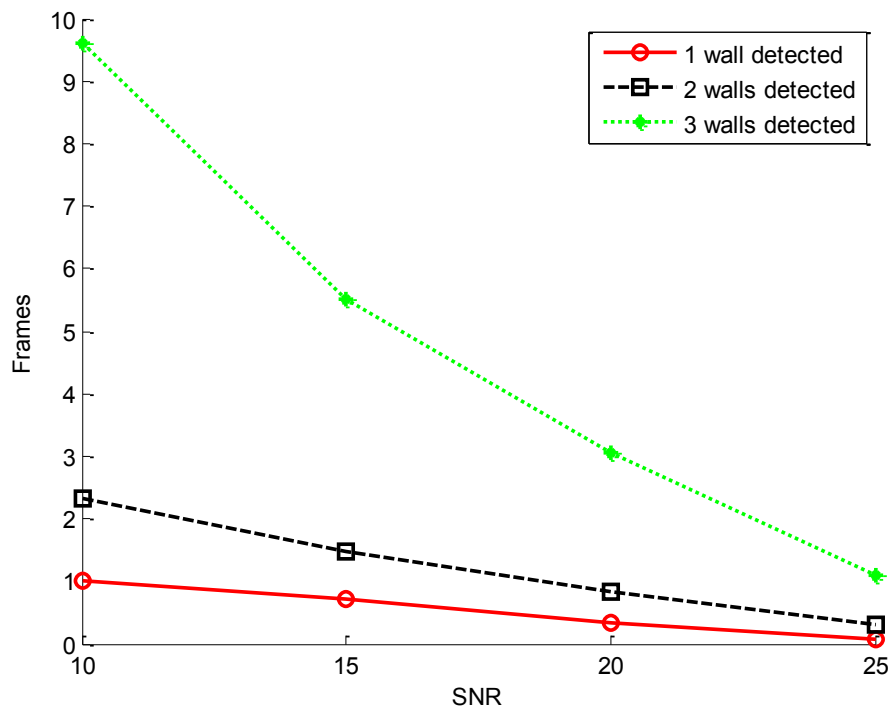


Figure 4.5: The average number of frames needed to achieve the success rate given in Figure 4.4 (a)

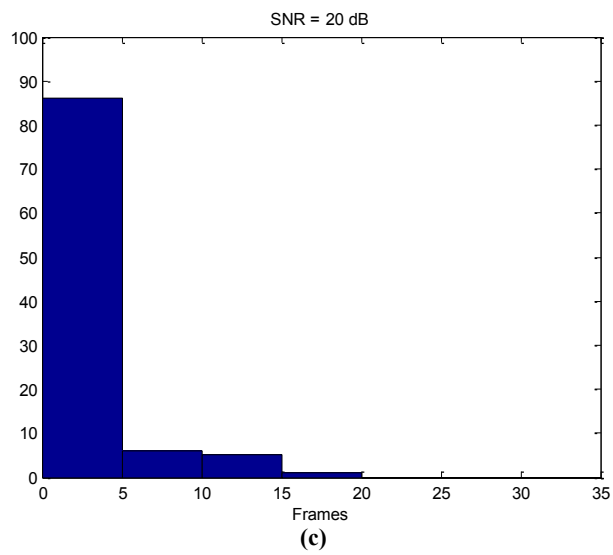
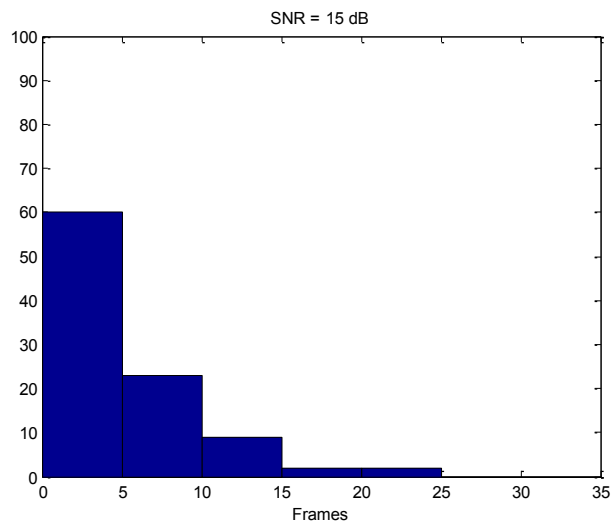
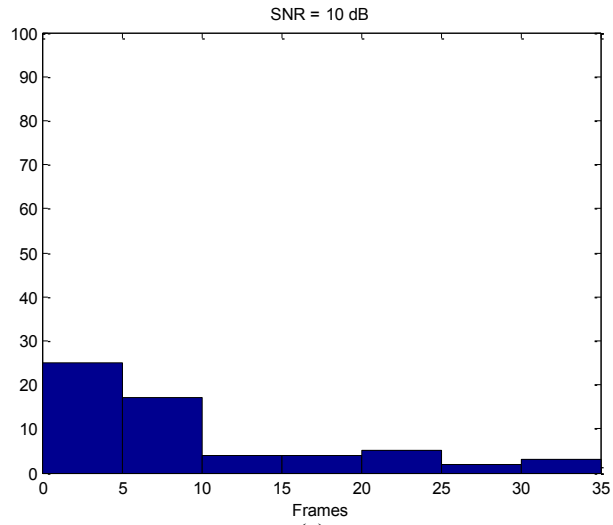


Figure 4.6: Histogram of number of frames needed for successful wall detection SNR = (a) 10, (b) 15, and (c) 20

4.6 Conclusion

This chapter introduced a general framework for jointly estimating the positions of the inner walls and reconstructing a ghost-free image of the given scene. Two algorithms within this framework were proposed. The second algorithm is a generalization of the first and utilizes the fact that moving targets increase the knowledge of the wall positions. The results show that making use of new information from different time frames play a significant role in increasing the overall performance of wall detection. The algorithm is able to detect the walls in less than 1 second, and in worst cases 5 seconds, when the SNR is higher than 15 *dB*.

CHAPTER 5: CONCLUSION AND RECOMMENDATIONS

5.1 Conclusion

In an attempt to find out which CS algorithm best suits TWRI, the first part of this thesis included a performance based comparison of a group of CS algorithms. The research contributions and collusions in this part can be summarized as follows:

1. **F_1 -score Performance Measure in CS:** We introduced a new method for assessing the detection capabilities of CS algorithms. It is based on the notion of F_1 -score, which allows us to quantitatively measure how well an algorithm is capable of detecting all the true targets without introducing any false ones.
2. **Performance Comparison of CS algorithms in TWRI:** Using the introduced performance measure, we compared the performance of 14 various CS algorithms after applying them to several TWRI scenarios. Different SNR values and reduction rates were considered in this comparison.

From this part, we specifically concluded the following:

- When the SNR is high, the algorithms performances are similar in most cases.
- In case of high SNR, discriminations between the algorithms arise when more than 90% reduction is required. In such cases, FPC and SPGL1 give the best performance.
- For low SNR values, YALL1 gives the best results in most cases.

In the second part of this thesis, we aimed at exploiting the multipath returns in order to enhance the image of the scene and suppress ghost targets. This part can be summarized as follows:

1. **Wall Pursuit (WP) Framework:** We developed a general framework for detecting the wall positions inside a room and obtaining a ghost-free image. The framework is based on parallel scans of the wall positions in each layer and gives each wall a cost. Information of the wall positions is shared between the layers through the multipath dictionary generator (MDG). This general framework sets the ground for a group of algorithms that are capable of detecting correct wall positions.
2. **"Basic" Wall Pursuit Algorithm:** We proposed an algorithm as an extension of the aforementioned general framework. At each layer, the wall position that produces the sparsest image is found and the dictionary is updated correspondingly and fed back to the layers to improve performance.

3. **Dynamic Wall Pursuit Algorithm:** We suggested making use of the presence of moving targets in gaining more information about the wall positions. The WP algorithm was extended on this basis. Moving targets were first detected using CD, then the same steps of WP algorithm were followed except that the cost values are accumulated and the level of depth is limited to a small value of D . This is repeated for several frames until the wall positions are detected.

The following conclusions are worth mentioning for this part:

- The Wall Pursuit algorithm works well in case of high SNR. However when the SNR decreases, the ability of the algorithms to detect all the true walls reduces significantly.
- When Dynamic Wall Pursuit is considered, detecting the correct wall positions is possible even with low SNR values.
- The number of frames needed to converge to the correct wall positions is usually less than five, for SNR above 15 dB .

5.2 Recommendations for Future Research

For further research, we recommend the following extensions:

1. Apart from the comparison presented, which concentrated on detection capabilities of the algorithms, other comparisons can be performed such as practicality of hardware realization, memory usage, processing time, and visual quality of the image.

2. In the proposed framework, no direct communication between the wall layers was taken into account during scanning. An improvement of the algorithm would be to allow direct on-line information transfer between the layers while scanning, instead of routing through the MPD.
3. In the WP algorithm, images of the scene are obtained using sparse reconstruction algorithms. However, these algorithms are time consuming. Simpler schemes for obtaining intermediate images, like back-projection, can be investigated with a proper cost function in order to get faster results.
4. In the DWP algorithm, the choice of depth, D , can be optimized to give better performance in the overall algorithm.
5. Modeling this problem probabilistically will help in accurately identifying which wall position is most probable.
6. The proposed algorithms can be further supported by providing theoretical formulations proving their convergence.
7. The structure of the dictionary should be utilized in order to improve the performance in terms of processing time and memory allocation.
8. The algorithm can be extended to work for irregular room geometry.

References

- [1] M. G. Amin, *Through-the-Wall Radar Imaging*, Boca Raton, FL: CRC Press, 2010.
- [2] F. Ahmad and M. Amin, "Through-the-Wall Human Motion Indication Using Sparsity-Driven Change Detection," *Geoscience and Remote Sensing, IEEE Transactions on* , vol. 51, no. 2, pp. 881,890, Feb. 2013.
- [3] M. Amin and F. Ahmad, "Change Detection Analysis of Humans Moving Behind Walls," *Aerospace and Electronic Systems, IEEE Transactions on*, vol. 49, no. 3, pp. 1410,1425, July 2013.
- [4] H. Wang, R. Narayanan and Z.-o. Zhou, "Through-Wall Imaging of Moving Targets Using UWB Random Noise Radar," *Antennas and Wireless Propagation Letters, IEEE* , vol. 8, pp. 802,805, 2009.
- [5] F. Soldovieri, R. Solimene and R. Pierri, "A simple strategy to detect changes in through the wall imaging," *Progress In Electromagnetics Research M*, vol. 7, pp. 1-13, 2009.
- [6] B. Lu, Q. Song, Z. Zhou and X. Zhang, "Detection of Human Beings in Motion Behind the Wall Using SAR Interferogram," *Geoscience and Remote Sensing*

Letters, IEEE, vol. 9, no. 5, pp. 968,971, Sept. 2012.

- [7] Q. Huang, L. Qu, B. Wu and G. Fang, "UWB Through-Wall Imaging Based on Compressive Sensing," *Geoscience and Remote Sensing, IEEE Transactions on*, vol. 48, no. 3, pp. 1408,1415, March 2010.
- [8] W. Zhang, M. G. Amin, F. Ahmad, A. Hoorfar and G. E. Smith, "Ultrawideband Impulse Radar Through-the-Wall Imaging with Compressive Sensing," *International Journal of Antennas and Propagation*, vol. 2012, p. 11, 2012.
- [9] R. Solimene, F. Ahmad and F. Soldovieri, "A Novel CS-TSVD Strategy to Perform Data Reduction in Linear Inverse Scattering Problems," *IEEE GEOSCIENCE AND REMOTE SENSING LETTERS*, vol. 9, no. 5, pp. 881 - 885, SEPTEMBER 2012.
- [10] F. Soldovieri, R. Solimene and F. Ahmad, "Experimental validation of a microwave tomographic approach for through-the-wall radar imaging," in *Proc. SPIE Defense and Security Symp.* vol. 7699, p. 76990C, 2010.
- [11] E. Lagunas, M. G. Amin, F. Ahmad and M. Nájar, "Joint Wall Mitigation and Compressive Sensing for Indoor Image Reconstruction," *IEEE TRANSACTIONS ON GEOSCIENCE AND REMOTE SENSING*, vol. 51, no. 2, pp. 891 - 906, FEBRUARY 2013.

- [12] B. Zhang and W. Wang, "Through-wall detection of human being with compressed UWB radar data," *EURASIP Journal on Wireless Communications and Networking* 2013, vol. 162, 2013.
- [13] E. Lagunas, M. G. Amin, F. Ahmad and M. Najjar, "Wall Mitigation Techniques for Indoor Sensing within the Compressive Sensing Framework," in *2012 IEEE 7th Sensor Array and Multichannel Signal Processing Workshop (SAM)*, 2012.
- [14] E. Lagunas, M. G. Amin, F. Ahmad and M. Nájjar, "Joint Wall Mitigation and Compressive Sensing for Indoor Image Reconstruction," *IEEE Transactions on Geoscience and Remote Sensing*, vol. 51, no. 2, pp. 891 - 906, Feb. 2013.
- [15] E. Lagunas, M. G. Amin, F. Ahmad and M. Najjar, "Sparsity-Based Radar Imaging of Building Structures," in *20th European Signal Processing Conference (EUSIPCO 2012)*, 2012.
- [16] E. Lagunas, M. G. Amin, F. Ahmad and M. Najjar, "Compressive Sensing for Through Wall Radar Imaging of Stationary Scenes Using Arbitrary Data Measurements," in *The 11th International Conference on Information Sciences, Signal Processing and their Applications: Special Sessions*, 2012.
- [17] E. Cristofani, M. Becquaert and M. Vandewal, "Performance of 2D Compressive Sensing on Wide-beam Through-the-wall Imaging," *Journal of Electrical and Computer Engineering*, vol. 2013, pp. 6:6--6:6, 2013.

- [18] H. Mansour and D. Liu, "Blind Multi-path Elimination by Sparse Inversion in Through-the-Wall-Imaging," *Computational Advances in Multi-Sensor Adaptive Processing (CAMSAP), 2013 IEEE 5th International Workshop on*, pp. 256,259, Dec. 2013.
- [19] M. Leigsnering, F. Ahmad, M. Amin and A. Zoubir, "Compressive sensing based specular multipath exploitation for through-the-wall radar imaging," *Acoustics, Speech and Signal Processing (ICASSP), 2013 IEEE International Conference on*, pp. 6004,6008, May 2013.
- [20] A. T. Abdalla, A. H. Muqaibel and a. S. Al-dharrab, "Aspect Dependent Multipath Ghost Suppression in TWRI under Compressive Sensing Framework," in *International Conference on Communications, Signal Processing and their Applications (ICCSPA15)*, 2015.
- [21] M. Duman and A. C. Gurbuz, "Performance analysis of compressive-sensing-based through-the-wall imaging with effect of unknown parameters," *International Journal of Antennas and Propagation*, vol. 2012, 2012.
- [22] J. Wang, P. Wang, Y. Li, Q. Song and Z. Zhou, "A multipath suppression technique for through-the-wall radar," in *Ultra-Wideband (ICUWB), 2013 IEEE International Conference on*, 2013.
- [23] F. Tivive, A. Bouzerdoum and V. H. Tang, "Multi-stage compressed sensing and wall clutter mitigation for through-the-wall radar image formation," in

Sensor Array and Multichannel Signal Processing Workshop (SAM), 2014 IEEE 8th, 2014.

- [24] Q. Huang, L. Qu, B. Wu and G. Fang, "UWB Through-Wall Imaging Based on Compressive Sensing," *Geoscience and Remote Sensing, IEEE Transactions on*, vol. 48, no. 3, pp. 1408,1415, Mar. 2010.
- [25] W. Zhang and A. Hoorfar, "A Generalized Approach for SAR and MIMO Radar Imaging of Building Interior Targets with Compressive Sensing," *Antennas and Wireless Propagation Letters, IEEE*, vol. PP, no. 99, pp. 1-1, 2015.
- [26] V. H. Tang, A. Bouzerdoum, S. L. Phung and F. H. C. Tivive, *Enhanced through-the-wall radar imaging using Bayesian compressive sensing*, vol. 8717, 2013, pp. 87170I-87170I-12.
- [27] P. Setlur, M. Amin and F. Ahmad, "Multipath Model and Exploitation in Through-the-Wall and Urban Radar Sensing," *Geoscience and Remote Sensing, IEEE Transactions on*, vol. 49, no. 10, pp. 4021,4034, Oct. 2011.
- [28] P. Setlur, G. Alli and L. Nuzzo, "Multipath Exploitation in Through-Wall Radar Imaging Via Point Spread Functions," *IEEE TRANSACTIONS ON IMAGE PROCESSING*, vol. 22, no. 12, pp. 4571-4586, DECEMBER 2013.
- [29] M. Leigsnering, F. Ahmad, M. Amin and A. Zoubir, "Compressive sensing based specular multipath exploitation for through-the-wall radar imaging,"

Acoustics, Speech and Signal Processing (ICASSP), 2013 IEEE International Conference on, pp. 6004,6008, 26-31 May 2013.

- [30] H. Mansour and D. Liu, "Blind Multi-path Elimination by Sparse Inversion in Through-the-Wall-Imaging," *Computational Advances in Multi-Sensor Adaptive Processing (CAMSAP), 2013 IEEE 5th International Workshop on*, pp. 256,259, 15-18 Dec. 2013.
- [31] G. Wang and M. Amin, "Imaging Through Unknown Walls Using Different Standoff Distances," *Signal Processing, IEEE Transactions on*, vol. 54, no. 10, pp. 4015-4025, Oct 2006.
- [32] G. Wang, M. Amin and Y. Zhang, "New approach for target locations in the presence of wall ambiguities," *Aerospace and Electronic Systems, IEEE Transactions on*, vol. 42, no. 1, pp. 301-315, Jan 2006.
- [33] F. Ahmad, M. Amin and G. Mandapati, "Autofocusing of Through-the-Wall Radar Imagery Under Unknown Wall Characteristics," *Image Processing, IEEE Transactions on*, vol. 16, no. 7, pp. 1785-1795, July 2007.
- [34] D. Donoho, "Compressed sensing," *Information Theory, IEEE Transactions on*, vol. 52, no. 4, pp. 1289-1306, April 2006.
- [35] E. Candes and T. Tao, "Near-Optimal Signal Recovery From Random Projections: Universal Encoding Strategies?," *Information Theory, IEEE*

Transactions on, vol. 52, no. 12, pp. 5406-5425, Dec 2006.

- [36] E. Candes, J. Romberg and T. Tao, "Robust uncertainty principles: exact signal reconstruction from highly incomplete frequency information," *Information Theory, IEEE Transactions on*, vol. 52, no. 2, pp. 489-509, Feb 2006.
- [37] E. Candes and M. Wakin, "An Introduction To Compressive Sampling," *Signal Processing Magazine, IEEE*, vol. 25, no. 2, pp. 21-30, March 2008.
- [38] M. Amin and F. Ahmad, "Change Detection Analysis of Humans Moving Behind Walls," *Aerospace and Electronic Systems, IEEE Transactions on*, vol. 49, no. 3, pp. 1410,1425, Jul. 2013.
- [39] P. Setlur, G. Alli and L. Nuzzo, "Multipath Exploitation in Through-Wall Radar Imaging Via Point Spread Functions," *IEEE Transactions on Image Processing*, vol. 22, no. 12, pp. 4571-4586, Dec. 2013.
- [40] S. Wright, R. Nowak and M. Figueiredo, "Sparse Reconstruction by Separable Approximation," *Signal Processing, IEEE Transactions on*, vol. 57, no. 7, pp. 2479-2493, July 2009.
- [41] J. Bioucas-Dias and M. Figueiredo, "A New TwIST: Two-Step Iterative Shrinkage/Thresholding Algorithms for Image Restoration," *Image Processing, IEEE Transactions on*, vol. 16, no. 12, pp. 2992-3004, Dec 2007.
- [42] J. Yang and Y. Zhang, "Alternating Direction Algorithms for l1-Problems in

- Compressive Sensing," *SIAM Journal on Scientific Computing*, vol. 33, no. 1, pp. 250-278, 2011.
- [43] Z. Wen, W. Yin, D. Goldfarb and Y. Zhang, "A Fast Algorithm for Sparse Reconstruction Based on Shrinkage, Subspace Optimization, and Continuation," *SIAM Journal on Scientific Computing*, vol. 32, no. 4, pp. 1832-1857, 2010.
- [44] E. Hale, W. Yin and Y. Zhang, "Fixed-Point Continuation for ℓ_1 -Minimization: Methodology and Convergence," *SIAM Journal on Optimization*, vol. 19, no. 3, pp. 1107-1130, 2008.
- [45] M. Figueiredo, R. Nowak and S. Wright, "Gradient Projection for Sparse Reconstruction: Application to Compressed Sensing and Other Inverse Problems," *Selected Topics in Signal Processing, IEEE Journal of*, vol. 1, no. 4, pp. 586-597, Dec 2007.
- [46] S.-J. Kim, K. Koh, M. Lustig, S. Boyd and D. Gorinevsky, "An Interior-Point Method for Large-Scale ℓ_1 -Regularized Least Squares," *Selected Topics in Signal Processing, IEEE Journal of*, vol. 1, no. 4, pp. 606-617, Dec 2007.
- [47] T. Blumensath and M. Davies, "Gradient Pursuits," *Signal Processing, IEEE Transactions on*, vol. 56, no. 6, pp. 2370-2382, June 2008.
- [48] E. van den Berg and M. Friedlander, "Probing the Pareto Frontier for Basis Pursuit Solutions," *SIAM Journal on Scientific Computing*, vol. 31, no. 2, pp.

890-912, 2009.

- [49] S. Babacan, R. Molina and A. Katsaggelos, "Bayesian Compressive Sensing Using Laplace Priors," *Image Processing, IEEE Transactions on*, vol. 19, no. 1, pp. 53-63, Jan 2010.
- [50] J. Tropp and A. Gilbert, "Signal Recovery From Random Measurements Via Orthogonal Matching Pursuit," *Information Theory, IEEE Transactions on*, vol. 53, no. 12, pp. 4655-4666, Dec 2007.
- [51] C. J. Van Rijsbergen, "Foundation of evaluation," *Journal of Documentation*, vol. 30, no. 4, pp. 365-373, 1974.
- [52] C. D. Manning and H. Schutze, *Foundations of statistical natural language processing*, MIT press, 1999.
- [53] I. Visentini, L. Snidaro and G. Foresti, "Selecting classifiers by F-score for real-time video tracking," in *Information Fusion (FUSION), 2010 13th Conference on*, 2010.
- [54] S. Heuel and H. Rohling, "Two-stage pedestrian classification in automotive radar systems," in *Radar Symposium (IRS), 2011 Proceedings International*, 2011.
- [55] J. Singh and M. Datcu, "Mining very high resolution complex-valued SAR images using the fractional Fourier transform," in *Synthetic Aperture Radar*,

2012. *EUSAR. 9th European Conference on*, 2012.

[56] M. Leigsnering, F. Ahmad, M. Amin and A. Zoubir, "CS based specular multipath exploitation in TWRI under wall position uncertainties," in *Sensor Array and Multichannel Signal Processing Workshop (SAM), 2014 IEEE 8th*, 2014.

[57] J.-F. Chen, W.-C. Lin, K.-H. Tsai and S.-Y. Dai, "Analysis and Evaluation of Human Movement based on Laban Movement Analysis," *Tamkang Journal of Science and Engineering*, vol. 14, no. 3, pp. 255-264, 2011.

Vitae

Ali AlBeladi

King Fahd University of Petroleum and Minerals

Electrical Engineering Department

E-Mail: albeladi@kfupm.edu.sa

Tel: +966 506 370020 (cell)

EDUCATION:

- 2013 - 2015 **Master of Science**, Electrical Engineering, King Fahd University of Petroleum and Minerals, Thesis title: "Multipath Exploitation in Through-Wall Radar Imaging Using Sparisty-Driven Change Detection"
- 2008 – 2012 **Bachelor of Science with First Honor**, Electrical Engineering, King Fahd University of Petroleum and Minerals.
- 2007 – 2008 **ARAMCO's College Preparatory Program**

EXPERIENCE:

- Sep. 2012 – 2015 **Graduate Assistant** at King Fahd University of Petroleum and Minerals, Teaching and coordinating the following laboratories:
- Digital Logic Design
 - Digital Systems Engineering
- Received the Exceptional Teaching Award (2014)
- Jan-May 2012 **Senior Project Group Leader**, "Implementing Near Field Communication (NFC) in KFUPM campus services"
- Jun-Aug 2011 **Summer Trainee**, Mobily Telecommunications Company, Transmission Department

BACKGROUND:

Major Courses taken:

- Digital Signal Processing, Compressive Sensing, Stochastic Process, Advanced Computer Vision, Communication Engineering 1&2, Microcontrollers & Embedded Systems, Telecommunication Networks, Satellite Communication, Industrial Instrumentation, RFID & Smart Cards.

RESEARCH INTERESTS:

- Digital Signal Processing
 - Radar Applications
 - Seismic Data Processing
 - Compressive Sensing Applications
- Artificial Intelligence and Robotics
- Digital VLSI System Design

TECHNICAL SKILLS:

MATLAB, Simulink, Verilog, JAVA, VHDL, PSpice, Assembly language, Latex, Microsoft Office (Microsoft Word, Excel, PowerPoint),